

Collinear fragmentation at NNLL: generating functionals, groomed correlators and angularities

Melissa van Beekveld,^a Mrinal Dasgupta,^{b,c} Basem Kamal El-Menoufi,^b Jack Helliwell,^a and Pier Francesco Monni^c

^a*Rudolf Peierls Centre for Theoretical Physics, Clarendon Laboratory, Parks Road, University of Oxford, Oxford OX1 3PU, UK*

^b*Lancaster-Manchester-Sheffield Consortium for Fundamental Physics, Department of Physics & Astronomy, University of Manchester, Manchester M13 9PL, United Kingdom*

^c*CERN, Theoretical Physics Department, CH-1211 Geneva 23, Switzerland*

E-mail: melissa.vanbeekveld@physics.ox.ac.uk,
mrinal.dasgupta@manchester.ac.uk, basem.el-menoufi@manchester.ac.uk,
jack.helliwell@physics.ox.ac.uk, pier.monni@cern.ch

ABSTRACT: Jet calculus offers a unique mathematical technique to bridge the area of QCD resummation with Monte Carlo parton showers. With the ultimate goal of constructing next-to-next-to-leading logarithmic (NNLL) parton showers we study, using the language of generating functionals, the collinear fragmentation of final-state partons. In particular, we focus on the definition and calculation of the Sudakov form factor, which physically describes the no-emission probability in an ordered branching process. We review recent results for quark jets and compute the Sudakov form factor for the collinear fragmentation of gluon jets at NNLL. The NNLL corrections are encoded in a z dependent two-loop anomalous dimension $\mathcal{B}_2(z)$, with z being a suitably defined longitudinal momentum fraction. This is obtained from the integration of the relevant $1 \rightarrow 3$ collinear splitting kernels combined with the one-loop corrections to the $1 \rightarrow 2$ counterpart. This work provides the missing ingredients to extend the methods of jet calculus in the collinear limit to NNLL and gives an important element of the next generation of NNLL parton shower algorithms. As an application we derive new NNLL results for both the fractional moments of energy-energy correlation FC_x and the angularities λ_x measured on mMDT/Soft-Drop ($\beta = 0$) groomed jets.

Contents

1	Introduction and motivation	2
2	Generating functionals for collinear fragmentation	3
2.1	Review of NLL resummation	3
2.2	Extension to the NNLL case	5
3	$\mathcal{B}_2^q(z)$ in the quark case and the physical coupling scheme	8
4	\mathcal{B}_2^g in the gluon case: definitions and computational strategy	9
5	Virtual corrections to $1 \rightarrow 2$ collinear splitting	11
6	Real $1 \rightarrow 3$ collinear splitting	13
6.1	The $C_{FT_R} n_f$ channel	15
6.2	The $C_{AT_R} n_f$ channel	16
6.3	The C_A^2 channel	18
7	Extraction of $\mathcal{B}_2^g(z)$	20
7.1	The $T_R^2 n_f^2$ channel	21
7.2	The $C_{FT_R} n_f$ channel	21
7.3	The $C_{AT_R} n_f$ channel	21
7.4	The C_A^2 channel	22
8	Moments of EEC and angularities in groomed jets at NNLL	23
9	Conclusions and Outlook	27
A	Leading order splitting functions	29
B	Expression of $\mathcal{B}_2(z)$ for quark fragmentation	30
C	The NNLL $\mathbb{K}^{\text{finite}}$ kernel	30
C.1	Quark fragmentation	30
C.2	Gluon fragmentation	32
D	Derivation of $\frac{\theta^2}{\sigma_0} \frac{d^2\sigma}{d\theta^2 dz}$	34
E	Double-soft end-point contributions to $\mathcal{B}_2^g(z)$	37

1 Introduction and motivation

In this paper and in a forthcoming article [1], we initiate a formulation of the methods of jet calculus [2–5] beyond the NLL order to describe the dynamics of collinear fragmentation. Jet calculus techniques, and specifically the generating functional method, stand out as a mathematical language to formulate self-similar branching processes. For this reason, they are particularly suitable to bridge the field of QCD resummation to that of parton shower Monte Carlo algorithms. This is an important direction to pursue in the context of improving the logarithmic accuracy of such algorithms for QCD phenomenology and is receiving widespread attention in the collider physics context (see e.g. Ref. [6] for an overview).

More specifically this work addresses the following points:

1. A large class of QCD resummations cannot be handled using purely analytic techniques since they do not admit a closed analytic form. This can be either due to the non-linear nature of the evolution equations (like for instance the resummation of microjet observables [7, 8], fragmentation [9–19] or non-global observables [20–30]) or to the high complexity of the observable which may not easily factorise in a suitable conjugate space (like for instance some complex event shapes or jet resolution parameters [31–33]). In such cases it is necessary to formulate the resummation in a way that can be solved accurately using numerical methods. The methods of jet calculus [2–5], notably Generating Functionals (GFs), offer a powerful mathematical tool to describe the resummation of logarithmic radiative corrections in collider observables, and constitute one avenue to achieve a numerical solution via Monte Carlo techniques.
2. The recent development of new techniques to construct parton- shower algorithms with demonstrable higher logarithmic accuracy (see e.g. Refs. [34–53]) offers an opportunity to further increase systematically their precision. The connection between these new developments in the area of parton showers and resummations is based on a well-defined set of accuracy criteria that are based directly on QCD dynamics (i.e. approximating correctly the real and virtual matrix elements in specific kinematical limits). Recent parton-shower algorithms [40, 42, 45, 46, 48–51, 53] are constructed in such a way that the above criteria are satisfied, hence achieving NLL accuracy for broad classes of observable at once. GFs help us push this important correspondence to a deeper level, by deriving evolution equations which provide an analytic connection between parton showers and all-order resummations. As a result, one can unify parton showers and resummations within a single framework, which allows for systematic developments in both areas simultaneously.

In this work we focus on the class of observables which feature only collinear sensitivity, and on the description of final state fragmentation, leaving the extension to initial state radiation to future work.¹

¹A related description of the evolution of soft radiation away from the collinear limit using the same

Here we calculate the analytical ingredients needed in the formulation of NNLL resummation within the GFs method. As we will demonstrate in forthcoming work [1], these ingredients can then also be used in Monte Carlo algorithms to correctly include virtual corrections,² which are not captured by the shower's unitary approximation. For this reason, ingredients of this type (such as the soft physical coupling scheme [54–56]) have to be computed in dimensional regularisation.

The aforementioned analytical ingredients amount to the anomalous dimensions defining the NNLL Sudakov form factor, which encodes the no-emission probability in the branching process, and is the back bone of both the GFs method and parton-shower algorithms. After reviewing the recent work of Ref. [57], which provides the NNLL Sudakov form factor for quark jets, here we frame these results in the context of the GFs method and furthermore define and compute the NNLL Sudakov form factor for the case of gluon fragmentation. We also discuss applications of our results in the context of QCD resummation, by deriving new NNLL accurate results for specific groomed jet observables related closely to those measured at the LHC. For these observables, the evolution equations can be solved in closed form and allows us to derive analytic results.

The layout of the paper is as follows. In Sec. 2 we introduce the Generating Functionals method as a way to understand the role of such analytic ingredients in a Monte Carlo calculation. We then discuss the extension to NNLL order in the collinear limit and define the NNLL Sudakov form factor and the anomalous dimension $\mathcal{B}_2(z)$. In Secs. 4–7 we calculate $\mathcal{B}_2^g(z)$ for gluon jets, which complements previous studies done for quark jets and discuss the important differences between these two cases. In Sec. 8 we provide concrete applications to collider phenomenology by deriving new results for the NNLL resummation of moments of energy-energy correlation [58] and angularities [59] measured on groomed jets with the mMDT/Soft-Drop procedure [60, 61]. Finally, we conclude in Sec. 9 and provide a number of appendices with additional technical details about the method and the calculations performed in this paper. The results for the $\mathcal{B}_2(z)$ anomalous dimensions for quarks and gluons are given in electronic format with the arXiv submission of this article.

2 Generating functionals for collinear fragmentation

In the present section we introduce the GF method to resum logarithmic corrections of collinear nature. We start by reviewing the NLL case and then we discuss the extension to NNLL.

2.1 Review of NLL resummation

We consider the collinear fragmentation of a parton of initial energy E resolved at an angular resolution $\theta \ll 1$. The all-order resummation at NLL resums single logarithms

mathematical language was discussed in Refs. [28, 29] in the context of non-global resummations in the large- N_c limit.

²Specifically, by unitary approximation we mean that in a parton shower virtual corrections simply amount to (minus) the integral of the real (soft and/or collinear) matrix element. This implies a unitary effect on the total cross section.

$L = -\ln \theta$ of the form $\alpha_s^n L^n$. At this order, the fragmentation can be formulated as a branching process in which emissions are strongly ordered in angle.³ At NNLL we aim at resumming corrections of order $\alpha_s^n L^{n-1}$, where now emissions can be unordered and have commensurate angles. To start, we therefore define an angular resolution scale t (evolution time) as

$$t_i = \int_{\theta_i^2}^1 \frac{d\theta^2}{\theta^2} \frac{\alpha_s(E^2 g^2(z) \theta^2)}{2\pi}, \quad (2.1)$$

where α_s is the $\overline{\text{MS}}$ coupling, and $g(z)$ is a function of the longitudinal momentum fraction $1 - z$ carried by the i -th emission. At NLL the precise form of $g(z)$ is irrelevant and one can set $g(z) = 1$ (see for example Ref. [7]). In what follows, the use of the $\beta(\alpha_s)$ function that drives the running of α_s at either one-loop or two-loop order, depending on whether the target accuracy is NLL or NNLL is understood.

We introduce the GF $G_f(x, t)$, which encodes the probability of resolving a fixed number of emissions in the time-like fragmentation of an initial parton of flavour $f \in \{q, g\}$ and momentum fraction x below a resolution angle set by an initial evolution time t . The GFs are defined in such a way that the probability of exclusively resolving m partons in the collinear fragmentation of a parton of flavour $f \in \{q, g\}$ and momentum fraction x starting at an evolution time t is given by [2, 4]

$$\int dP_m^{(f)} = \frac{1}{m!} \frac{\delta^m}{\delta u^m} G_f(x, t) \Big|_{\{u\}=0}. \quad (2.2)$$

The quantity $u \equiv u(x, t; f)$ is the *probing function* and has the role of tagging a real emission in the functional derivative of G_f . Eq. (2.2) can be taken as the definition of the generating functional G_f . The evolution of the GFs with the resolution scale t is described, at NLL, by the coupled system of integral equations [7]⁴

$$\begin{aligned} G_q(x, t) &= u \Delta_q(t) + \int_t^{t_0} dt' \int_{z_0}^{1-z_0} dz P_{qq}(z) G_q(x z, t') G_g(x(1-z), t') \frac{\Delta_q(t)}{\Delta_q(t')}, \\ G_g(x, t) &= u \Delta_g(t) + \int_t^{t_0} dt' \int_{z_0}^{1-z_0} dz \left[P_{gg}(z) G_g(x z, t') G_g(x(1-z), t') \right. \\ &\quad \left. + P_{qg}(z) G_q(x z, t') G_q(x(1-z), t') \right] \frac{\Delta_g(t)}{\Delta_g(t')}, \end{aligned} \quad (2.3)$$

where t_0 is a collinear cutoff at which the evolution stops, while z_0 is an infrared cutoff on the energy fraction of each emission, which must be taken to zero in the calculation of an IRC safe observable (unlike for z_0 , the value of t_0 is bounded by the presence of the

³Angular ordering ensures the full coverage of the relevant phase space at NLL. Beyond NLL, emissions can have commensurate angles and therefore the precise definition of angular ordering (i.e. with respect to a specific reference direction) has to be specified in order to guarantee the coverage of the full phase space.

⁴An equivalent differential form can be easily obtained by dividing G_f by Δ_f and subsequently taking the t derivative. Note that Ref. [7] adopts a slightly different definition of the GFs which in this reference describe the fragmentation of a parton from a starting time $t = 0$ down to a resolution angle set by the time t . This convention is complementary to the one adopted in this paper, but their difference is irrelevant at the level of physical results.

Landau pole). The standard leading-order splitting functions are given in Appendix A. The above set of equations can be used to derive collinear resummations with NLL (single logarithmic) accuracy for final state radiation.

The Sudakov form factors Δ_f describe the no-emission probability and can be derived by imposing the unitarity condition

$$G_f(x, t)|_{u=1} = 1, \quad (2.4)$$

from which one obtains

$$\ln \Delta_q(t) = - \int_t^{t_0} dt' \int_{z_0}^{1-z_0} dz P_{qq}(z), \quad (2.5)$$

$$\ln \Delta_g(t) = - \int_t^{t_0} dt' \int_{z_0}^{1-z_0} dz (P_{gg}(z) + P_{qg}(z)). \quad (2.6)$$

An obvious boundary condition is then $G_f(x, t_0) = u$, indicating a 100% probability of finding a parton f with momentum x . With the above definition of the GFs, the resummed distribution (or equivalently cumulative distribution) $d\sigma^{(f)}$ for a given observable $v = V(\{k_i\})$ (with $\{k_i\}$ denoting the final state momenta produced in the fragmentation of a jet of initial flavour f) has the general form

$$d\sigma^{(f)} = \sigma_0 C(\alpha_s) \otimes J^{(f)}(\alpha_s, v), \quad (2.7)$$

where σ_0 is the Born cross section for the hard process under consideration. The jet distribution $J^{(f)}$ is simply obtained by integrating Eq. (2.2) with the measurement function of the observable for any final-state multiplicity m , that is

$$J^{(f)}(\alpha_s, v) = \sum_{m=1}^{\infty} \int dP_m^{(f)} \delta(v - V(\{k\}_m)). \quad (2.8)$$

The \otimes operation is observable dependent. It is usually a regular product, but for some specific observables (e.g. fragmentation functions) it can take the form of a convolution over the longitudinal momentum fraction. The process- and observable-dependent matching coefficient $C(\alpha_s)$ admits a fixed-order perturbative expansion in powers of the strong coupling constant $C(\alpha_s) = 1 + \mathcal{O}(\alpha_s)$, and it accounts for constant terms stemming from the matching of the jet distribution (defined by the GFs evolution equation) to the fixed order QCD calculation in the limit $v \rightarrow 0$. Specifically, at NNLL $C(\alpha_s)$ is required at the one-loop order, which entails the difference between the full $\mathcal{O}(\alpha_s)$ QCD calculation in the logarithmic limit (i.e. $v \rightarrow 0$) for the observable v and the expansion of the jet function at the same order.

2.2 Extension to the NNLL case

The extension of the above formulation to NNLL order requires the generalisation of the r.h.s. of the evolution equations (2.3) to $\mathcal{O}(\alpha_s^2)$. To understand what the calculation entails, we observe that Eqs. (2.3) describe the fragmentation by a sequence of angular ordered branchings. The resulting emission probability is the iteration of $1 \rightarrow 2$ splitting kernels, an

independent emission pattern, which correctly describes the NLL strongly ordered regime, i.e. $t_i \ll t_{i+1}$. At NNLL one needs to account for unordered corrections, i.e. $t_i \sim t_{i+1}$, which are described by the full set of $1 \rightarrow 3$ splitting kernels [62–64]. Such a correction will generate an extra term in Eqs. (2.3) which contains a product of three GFs (e.g. the splitting $q \rightarrow qgg$ will be proportional to $G_q G_g G_g$). At the same time one has to consider the virtual one-loop corrections to the $1 \rightarrow 2$ splitting kernels [65], which will have the same GFs structure as the NLL kernel (2.3). Finally, to avoid double counting with the $\mathcal{O}(\alpha_s^2)$ iteration of the NLL evolution, we must subtract the latter from the r.h.s. of Eqs. (2.3).

The aforementioned calculation can be consistently performed in the dimensional regularisation scheme in $d = 4 - 2\epsilon$ dimensions. However, in order to exploit the flexibility of Monte Carlo integration, we need to bring the integral equations into a form that is manifestly finite so that we can take $\epsilon \rightarrow 0$ at the integrand level. In order to make the cancellation of ϵ divergences manifest, we include a local subtraction term with the goal of regularising both the $1 \rightarrow 3$ real and $1 \rightarrow 2$ virtual corrections. The subtraction can be built directly from the $1 \rightarrow 3$ real corrections, by integrating them with the same $1 \rightarrow 2$ GFs structure present in the NLL kernel (2.3). In the reals, this effectively plays the role of a virtual correction obtained by unitarity. This procedure results in evolution equations that are manifestly finite in four space time dimensions. In the case of quark jets, the NNLL evolution equation takes the form

$$G_q(x, t) = u \Delta_q(t) + \int_t^{t_0} dt' \int_{z_0}^{1-z_0} dz G_q(x z, t') G_g(x(1-z), t') \frac{\Delta_q(t)}{\Delta_q(t')} \mathcal{P}_q(z, \theta) + \mathbb{K}_q^{\text{finite}}[G_q, G_g]. \quad (2.9)$$

In the above equation we defined the *inclusive emission probability* $\mathcal{P}_q(z, \theta)$ as⁵

$$\mathcal{P}_q(z, \theta) \equiv \frac{2 C_F}{1-z} \left(1 + \frac{\alpha_s(E^2 g^2(z) \theta^2)}{2\pi} K^{(1)} \right) + \mathcal{B}_1^q(z) + \frac{\alpha_s(E^2 g^2(z) \theta^2)}{2\pi} (\mathcal{B}_2^q(z) + \mathcal{B}_1^q(z) b_0 \ln g^2(z)), \quad (2.10)$$

where θ is the angle between the final state quark and gluon (set by the evolution time t'). The inclusive emission probability $\mathcal{P}_q(z)$ (and its gluonic counterpart) will be also central to the construction of an algorithmic solution to the NNLL problem, as we shall demonstrate in forthcoming work [1]. The quantity $K^{(1)}$ is the ratio of the two-loop to the one-loop cusp anomalous dimension

$$K^{(1)} = \left(\frac{67}{18} - \frac{\pi^2}{6} \right) C_A - \frac{10}{9} T_R n_f \equiv K^{(1), C_A} C_A + K^{(1), n_f} T_R n_f, \quad (2.11)$$

and b_0 is the first coefficient of the QCD beta function

$$b_0 = \frac{11}{6} C_A - \frac{2}{3} T_R n_f \equiv b_0^{(C_A)} C_A + b_0^{(n_f)} T_R n_f. \quad (2.12)$$

⁵The precise form of $g(z)$ in the coefficient of $\mathcal{B}_2^q(z)$ is not relevant at NNLL, but we keep it in for simplicity.

We have further decomposed the splitting function $P_{qq}(z)$ into its soft part ($z \simeq 1$) and the hard-collinear left over, where the latter is given by

$$\mathcal{B}_1^q(z) \equiv -C_F(1+z). \quad (2.13)$$

The term proportional to $b_0 \ln^2 g(z)$ balances the $g(z)$ dependence of the argument of the overall coupling encoded in dt' in Eq. (2.14), such that the quantity $\mathcal{B}_2^q(z)$ is independent of the choice of $g(z)$ and matches the definition and calculation given in Ref. [57]. The definition of $\mathcal{P}_q(z, \theta)$ implicitly relies upon a scheme to define the variables z and θ while integrating over a second emission (and adding the corresponding virtual corrections). This scheme must be IRC safe and effectively $\mathcal{P}_q(z, \theta)$ can be thought of as a next-to-leading-order correction to a $1 \rightarrow 2$ collinear splitting.

The functional $\mathbb{K}_q^{\text{finite}}$ contains 4-dimensional terms which can be handled efficiently with Monte Carlo methods.⁶ These terms satisfy a unitarity condition $\mathbb{K}_q^{\text{finite}}|_{u=1} = 0$, they are at most NNLL ($\alpha_s^n L^{n-1}$) and contain structures of the $G_i G_j G_k$ type. Although in the most general case they enter in NNLL resummations, for event shapes and jet rates they only enter in the soft limit and are responsible for correlated and clustering corrections in the language of Refs. [32, 33, 55, 66, 67]. On the other hand, for purely collinear problems, such as the dynamics of small- R jets [7], $\mathbb{K}_q^{\text{finite}}$ contributes as a whole. The precise definition of $\mathbb{K}_q^{\text{finite}}[G_q, G_g]$ goes hand-in-hand with the definition of the function \mathcal{B}_2^q , of which it specifies the scheme. Nevertheless, any physical prediction is independent of such a scheme, and for any IRC safe observables the scheme change can be performed directly in $d = 4$ dimensions. We report the expressions of such terms for quark and gluon jets in Appendix C, while in the body of this article we focus on the first line of Eq. (2.9) and its gluonic counterpart.

The function $\mathcal{B}_2^q(z)$ was calculated recently in Ref. [57] and will be reviewed in the next section. One can now define the Sudakov $\Delta_q(t)$ at NNLL from Eq. (2.9). We can set $u = 1$ and obtain

$$\ln \Delta_q(t) = - \int_t^{t_0} dt' \int_{z_0}^{1-z_0} dz \mathcal{P}_q(z, \theta). \quad (2.14)$$

The goal of this article is to define and calculate the analogous quantity for gluon jets $\mathcal{B}_2^g(z)$, which paves the way to obtain the Sudakov for the gluon fragmentation and the complete set of integral equations which generalises jet calculus in the collinear limit to NNLL.

Finally, the function $g(z)$ fixes the precise scale of the coupling that becomes relevant at NNLL. An important constraint on $g(z)$ is that in the soft limit ($z \simeq 1$) it is fixed to [54]

$$\lim_{z \rightarrow 1} \frac{g(z)}{1-z} = 1, \quad (2.15)$$

so that the coupling is evaluated at the relative transverse momentum of the branching. Beyond the soft limit, the form of $g(z)$ and $\mathcal{B}_2(z)$ are linked and emerge from an $\mathcal{O}(\alpha_s^2)$

⁶The application of this formalism to collinear unsafe quantities, such as fragmentation functions, entails considerable conceptual subtleties [1].

calculation. For the sake of concreteness, in the rest of this article we take

$$g(z) = 1 - z. \quad (2.16)$$

This defines unambiguously the terms in $\mathcal{B}_2(z)$ that are proportional to the QCD $\beta(\alpha_s)$ function at one loop (i.e. b_0).

3 $\mathcal{B}_2^q(z)$ in the quark case and the physical coupling scheme

In this section we give a concise review of the results for quark jets in Ref. [57]. This helps elucidate the main messages of the current work, in addition to showcasing some differences to the case of gluon jets. In the inclusive emission probability for quark jets (2.10), the intensity of radiation in the soft limit ($z \simeq 1$) can be encoded in a physical scheme of the strong coupling constant [54], in such a way that the emission probability is defined as

$$dt dz \mathcal{P}_q(z, \theta)|_{\text{soft}} \simeq C_F \frac{d\theta^2}{\theta^2} dz \frac{2}{1-z} \frac{\alpha_s^{\text{CMW}}(E^2(1-z)^2\theta^2)}{2\pi}, \quad (3.1)$$

where the r.h.s. amounts to using the first line of Eq. (2.10) and the CMW coupling is related to the $\overline{\text{MS}}$ one by the following relation

$$\alpha_s^{\text{CMW}}(\mu^2) = \alpha_s(\mu^2) \left(1 + \frac{\alpha_s(\mu^2)}{2\pi} K^{(1)} \right). \quad (3.2)$$

The above scheme is customarily used in QCD resummations and is a crucial analytical ingredient for NLL parton shower algorithms.

The extension of this picture to higher logarithmic accuracy is not unique, and depends on the definition of the kinematic variables z and θ . While generalisations of Eq. (3.2) to three loops (encoded in the coefficient $K^{(2)}$) in the soft limit (relevant for double-logarithmic resummations) were obtained in Refs. [55, 56], much less is known about its generalisation to the hard-collinear limit. In resummation literature this information is encoded, at the integrated level, in the *observable-dependent* collinear anomalous dimension commonly known as B_2 , which nowadays has been calculated for several observables [55, 68–70]. When used in resummations of double logarithmic observables such as event shapes or transverse momentum of a colour singlet, B_2 always takes the form (see e.g. Refs. [55, 68–70])

$$B_2^q = -\gamma_q^{(2)} + b_0 X, \quad (3.3)$$

where $\gamma_q^{(2)}$ is the endpoint of the singlet DGLAP splitting kernel at two loops (e.g. [5])

$$\gamma_q^{(2)} = C_F^2 \left(\frac{3}{8} - \frac{\pi^2}{2} + 6\zeta_3 \right) + C_F C_A \left(\frac{17}{24} + \frac{11\pi^2}{18} - 3\zeta_3 \right) - T_R n_f \left(\frac{1}{6} + \frac{2\pi^2}{9} \right), \quad (3.4)$$

and the quantity X is observable dependent.

Eq. (2.14) however suggests that we can encode this observable dependence into the *observable-independent* inclusive emission probability $\mathcal{P}_q(z, \theta)$, which encapsulates a differential anomalous dimension $\mathcal{B}_2^q(z)$. The observable dependence of B_2 thus emerges entirely

from the integration over z , and specifically from integrating the Sudakov (2.14) with the *single-emission* measurement function parameterised in terms of z and θ , i.e.⁷

$$\Theta(V(z, \theta) - v). \quad (3.5)$$

This offers a natural path to incorporate this information in Monte Carlo parton showers, and it constitutes a crucial step towards the development of NNLL algorithms. Recently, Ref. [57] presented a two loop calculation of the quantity $\mathcal{B}_2^q(z)$ in Eq. (2.14) for the quark case, where the corresponding $1 \rightarrow 3$ splitting kernels are integrated by fixing z and θ to the momentum fraction and angle of either the first emission, i.e. the one at larger angles for the C_F^2 channel, or that of the radiated pair (for the $C_F C_A$, $T_R n_f$ and $C_F (C_F - C_A/2)$ channels).⁸ Its expression is given in Appendix B.

The differential anomalous dimension $\mathcal{B}_2^q(z)$ is sufficient to derive B_2 for any rIRC safe global observable defined on quark jets (see also the related discussions in Section 3 of Ref. [57]). Specifically, for the definition of z and θ adopted in Ref. [57] (and reported in Appendix B) one obtains

$$\int_0^1 dz \mathcal{B}_2^q(z) \equiv B_{2,\theta^2}^q = -\gamma_q^{(2)} + b_0 X_{\theta^2}^q, \quad (3.6)$$

where

$$X_{\theta^2}^q = C_F \left(\frac{2\pi^2}{3} - \frac{13}{2} \right). \quad (3.7)$$

An analogous integration taking into account the observable constraint (3.5) would produce the observable-specific constant X . Explicit examples of this will be considered in Sec. 8.

4 \mathcal{B}_2^q in the gluon case: definitions and computational strategy

To calculate $\mathcal{B}_2^g(z)$, one needs an IRC safe definition of z and θ such that it projects the $1 \rightarrow 3$ phase space Φ_3 onto the underlying $1 \rightarrow 2$ kinematics Φ_2 . The definition of $\mathcal{B}_2^g(z)$ is then uniquely specified by a kinematical map

$$\mathcal{M} : \Phi_3 \rightarrow \Phi_2, \quad (4.1)$$

that provides a definition of the longitudinal momentum fraction z and the angle θ of the first branching in the Φ_2 phase space. This also defines in a unique manner the inclusive emission probability $\mathcal{P}(z, \theta)$, where one integrates over a second emission while keeping the variables z and θ fixed. A property of the definition of z and θ is that this projection reproduces $K^{(1)}$ in the soft limit. The generalisation of the calculation of the quark case [57] to the gluonic case is non-trivial and it entails two conceptual subtleties:

⁷We note that some definitions of the B_2^q coefficient (and thus of z and θ) in the literature contain an extra contribution arising from single-logarithmic soft physics (see e.g. Ref. [55]). These terms do not contribute to B_2^q in our scheme for quark jets, and they emerge from the integration of the $\mathbb{K}_q^{\text{finite}}[G_q, G_g]$ contribution. We will return to this point when discussing the case of gluon jets.

⁸The definition of the radiated pair is ambiguous in the $C_F (C_F - C_A/2)$ colour channel due to the symmetry of the splitting kernel, however this ambiguity does not affect the form of $\mathcal{B}_2^q(z)$.

1. In the case of quark jets it was possible to define z and θ based on the colour structure of the triple collinear matrix elements. Specifically, independent (i.e. C_F^2) and correlated (i.e. $C_F C_A$, $C_F T_R$, and $C_F (C_F - C_A/2)$) channels are separated by their colour structure. This allows one to choose z and θ such that in the abelian channel (C_F^2) these correspond to the kinematics of the first emission in an angular ordered picture, while in the remaining channels these variables correspond to the kinematics of the *parent* emitter of the final state pair of real partons (see e.g. Fig. 7). In the gluonic case, and specifically for the C_A^2 piece, this correspondence between independent and correlated emissions and different colour channels is no longer valid, in that independent and correlated radiation are mixed under the same colour structure. As a result, we need to formulate an IRC safe procedure to define z and θ in all gluonic channels.
2. A second subtlety concerns the flavour structure and the divergences in the gluonic case, which is more involved than in the quark case as reflected in the evolution equation for the gluonic GF (2.3). Unlike in the quark case, the gluon GF encodes two different splitting kernels already at NLL. Of these, $p_{gg}(z)$ is such that in an iterated $1 \rightarrow 2$ splitting $g \rightarrow g_a(z)g_b(1-z)$ followed by, e.g., $g_b \rightarrow q\bar{q}$ the gluon g_a which does not branch can still bring a soft divergence (this time at $z \simeq 0$). This behaviour is absent in the quark case (as $z \rightarrow 0$ would correspond to a soft quark configuration), and ensuring the cancellation of all IRC divergences in the gluon case requires a definition of the underlying $1 \rightarrow 2$ branching that is safe in this limit.

We give below a definition of z and θ that addresses the above features and can be used to derive $\mathcal{B}_2^g(z)$. The procedure follows a strategy inspired by the mMDT/Soft-Drop ($\beta = 0$) algorithm [60, 61] which was designed to identify hard-collinear splittings in a jet. It can be summarised in the following steps:

- For each colour channel, decompose the phase space into angular sectors, such that each sector contains exactly one collinear singularity. Evidently, the number of required sectors matches the number of singular collinear configurations in each colour channel.
- For each sector, we cluster the two partons, say i and j , which give rise to the collinear singularity as $\theta_{ij} \rightarrow 0$.
- In each sector the angle θ is identified with the angle between the clustered pair (ij) and the remaining parton k . Similarly, the longitudinal momentum fraction z coincides with that of parton k , i.e. $z \equiv z_k$. We then symmetrise the result by adding the permutation $z \rightarrow 1 - z$ and multiply by $1/2!$ if the Born $1 \rightarrow 2$ splitting to which we are projecting involves identical particles. The procedure follows the angular-ordered pattern of the generating functional evolution equation.
- In the region of phase space where $z_k \rightarrow 0$, the definition of the angle θ becomes unsafe. Therefore, when z_k is below a certain threshold, say $z_{\text{cut}} \ll 1$, we discard

the soft branch containing z_k and fix the angle $\theta \equiv \theta_{ij}$. In addition the longitudinal momentum is chosen as $z \equiv z_i/(z_i+z_j)$ which must necessarily pass the z_{cut} condition in order to define a hard-collinear splitting.

- Finally, we explicitly take the limit $z_{\text{cut}} \rightarrow 0$.

In practice we consider the fragmentation of a gluon jet defined as one hemisphere in the two-jet limit of the $H \rightarrow gg$ decay in the heavy-top-mass limit. The corresponding NNLL resummed doubly-differential distribution in z and θ is given in Eq. (D.13) of Appendix D. The extraction of $\mathcal{B}_2^g(z)$ then can proceed by simply relating the second order calculation for $\frac{\theta^2}{\sigma_0} \frac{d^2\sigma}{d\theta^2 dz}$ to the second order expansion of Eq. (D.13). In general our procedure is not exactly the same as mMDT⁹ since it does not correspond to the exact C/A declustering sequence. Yet, our clustering sequence is sufficient to capture all the divergent structure and obtain an IRC safe effective emission probability.

In contrast to the quark case, in which the integral of $\mathcal{B}_2^q(z)$ yields the simple form given in Eq. (3.6), the richer singularity structure present in the gluon case (specifically in the C_A^2 channel) and reflected in the emergence of multiple singular sectors as outlined above will lead to the general form

$$\int_0^1 \mathcal{B}_2^g(z) \equiv B_{2,\theta^2}^g = -\gamma_g^{(2)} + b_0 X_{\theta^2}^g + \mathcal{F}_{\text{clust.}}^{C_A^2}, \quad (4.2)$$

where [5]

$$-\gamma_g^{(2)} = \frac{4}{3} C_A T_R n_f + C_F T_R n_f - C_A^2 \left(\frac{8}{3} + 3\zeta_3 \right), \quad (4.3)$$

and $X_{\theta^2}^g$ is a constant that we shall determine in Sec. 7. Finally, the extra term $\mathcal{F}_{\text{clust.}}^{C_A^2}$ emerges from the non-trivial sectorisation that becomes necessary in the C_A^2 channel (cf. Sec. 7.4).

In the next sections we discuss how to use the above algorithm to define and calculate the inclusive emission probability $\mathcal{P}_g(z, \theta)$. In particular, in order to calculate $\mathcal{P}_g(z, \theta)$ we start by computing the doubly-differential distribution $\theta^2 d^2\sigma/d\theta^2 dz$, and then in Sec. 7 we will extract $\mathcal{P}_g(z, \theta)$. We will discuss separately the contribution of the one-loop correction to the collinear $1 \rightarrow 2$ splitting kernel and of the tree-level $1 \rightarrow 3$ splitting kernels.

5 Virtual corrections to $1 \rightarrow 2$ collinear splitting

We start by discussing the $\mathcal{O}(\alpha_s^2)$ real-virtual corrections to the $\theta^2 d^2\sigma/d\theta^2 dz$ distribution. We parameterise them as follows:

$$\left(\frac{\theta^2}{\sigma_0} \frac{d^2\sigma_{\mathcal{V}}^{(2)}}{d\theta^2 dz} \right) = \left(\frac{\alpha_s}{2\pi} \right)^2 \mathcal{V}(\theta^2, z, \epsilon), \quad (5.1)$$

where, in this case, the kinematical variables (θ, z) are uniquely defined as those of a $1 \rightarrow 2$ collinear splitting. Our results will be expressed in terms of a renormalised $\overline{\text{MS}}$ coupling

⁹An exception is given by the C_A^2 channel, where our procedure is equivalent to the mMDT algorithm.

related to the bare strong coupling by

$$\mu^{2\epsilon} \alpha_s = S_\epsilon^{-1} \mu_R^{2\epsilon} \alpha_s(\mu_R^2) \left(1 - \frac{b_0}{\epsilon} \frac{\alpha_s(\mu_R)}{2\pi} + \mathcal{O}(\alpha_s^2) \right), \quad (5.2)$$

where

$$S_\epsilon = (4\pi)^\epsilon e^{-\epsilon\gamma_E}. \quad (5.3)$$

Finally, we choose $\mu_R = E$ (the energy of the hard parton initiating the fragmentation) to present the results, and define $\alpha_s \equiv \alpha_s(E^2)$. There are three kinds of one-loop corrections that are involved in the calculation, and they can be separated according to their origin. The first is the one-loop UV counter-term that is related to the renormalisation of the bare coupling (5.2), and reads:

$$\mathcal{V}_{\text{renorm.}}(\theta^2, z, \epsilon) = -\frac{b_0}{\epsilon} (z(1-z)\theta)^{-2\epsilon} (C_A p_{gg}(z) + T_R n_f p_{qg}(z, \epsilon)). \quad (5.4)$$

The second is the one-loop correction to the $1 \rightarrow 2$ splitting function itself. These corrections are taken from Ref. [65], in the CDR scheme.¹⁰ Explicitly, the one-loop correction to the collinear $g \rightarrow q\bar{q}$ splitting is given by

$$\begin{aligned} \mathcal{V}_{g \rightarrow q\bar{q}}^{(1)}(\theta^2, z, \epsilon) &= (z(1-z))^{-3\epsilon} \theta^{-4\epsilon} T_R n_f p_{qg}(z, \epsilon) \left(\frac{1}{\epsilon^2} - \frac{2\pi^2}{3} \right) \times \\ &\quad \times \left[T_R n_f f_{T_R n_f}^{g \rightarrow q\bar{q}} + C_F f_{C_F}^{g \rightarrow q\bar{q}} + C_A f_{C_A}^{g \rightarrow q\bar{q}} \right], \end{aligned} \quad (5.5)$$

where

$$f_{T_R n_f}^{g \rightarrow q\bar{q}} = -\frac{4\epsilon}{3} - \frac{20\epsilon^2}{9} + \mathcal{O}(\epsilon^3), \quad (5.6)$$

$$f_{C_F}^{g \rightarrow q\bar{q}} = -2 - 3\epsilon - 8\epsilon^2 + \mathcal{O}(\epsilon^3), \quad (5.7)$$

$$f_{C_A}^{g \rightarrow q\bar{q}} = 1 + \frac{11\epsilon}{3} + \frac{76\epsilon^2}{9} + \epsilon \ln(z(1-z)) + \epsilon^2 \text{Li}_2\left(\frac{z-1}{z}\right) + \epsilon^2 \text{Li}_2\left(\frac{z}{z-1}\right) + \mathcal{O}(\epsilon^3). \quad (5.8)$$

For the one-loop correction to the collinear $g \rightarrow gg$ splitting we have

$$\mathcal{V}_{g \rightarrow gg}^{(1)}(\theta^2, z, \epsilon) = (z(1-z))^{-3\epsilon} \theta^{-4\epsilon} C_A^2 p_{gg}(z, \epsilon) \left(\frac{1}{\epsilon^2} - \frac{2\pi^2}{3} \right) f_{C_A}^{g \rightarrow gg} + \frac{1}{6} C_A^2 - \frac{1}{3} C_A T_R n_f, \quad (5.9)$$

where

$$f_{C_A}^{g \rightarrow gg} = -1 + \epsilon \ln(z(1-z)) + \epsilon^2 \text{Li}_2\left(\frac{z-1}{z}\right) + \epsilon^2 \text{Li}_2\left(\frac{z}{z-1}\right) + \mathcal{O}(\epsilon^3). \quad (5.10)$$

¹⁰In the $T_R^2 n_f^2$ channel, we noticed a typographical error in Eq. (5.19) of the journal version of Ref. [65], which we fix to recover the divergent structure predicted by Catani's one-loop formula [71]. Specifically, one should replace -3 with $+3$ in the denominator of the first term on the r.h.s. of Eq. (5.19) in the journal version of Ref. [65].

We finally note that if we were to compute the full $\mathcal{O}(\alpha_s^2)$ result for a given observable then the one-loop virtual corrections to the Born process would also have to be included. In practice, for the double-differential calculation at second order that we carry out here only the product of such one-loop virtual corrections with the single collinear splitting function is needed. For the $H \rightarrow gg$ process in the heavy-top effective theory considered in this article it reads (with $\mu_R = E$)

$$\begin{aligned} \mathcal{V}_{H \rightarrow gg}^{(1)\text{Born}}(\theta^2, z, \epsilon) &= (C_A p_{gg}(z) + T_R n_f p_{qg}(z, \epsilon)) \left(1 - \frac{\pi^2}{12}\epsilon^2\right) (z^2(1-z)^2\theta^2)^{-\epsilon} \\ &\times \left(\left(-\frac{4^{-\epsilon}}{\epsilon^2} - \frac{11}{6\epsilon} + \frac{7}{12}\pi^2 \right) C_A + \frac{2}{3\epsilon} T_R n_f \right). \end{aligned} \quad (5.11)$$

In the above expression, the process dependence is embodied in the $\mathcal{O}(\epsilon^0)$ terms of the above equation, and it cancels in the extraction of $\mathcal{B}_2^g(z)$ when taking the difference between our second-order calculation and the expansion of the resummation formula given in Eq. (D.13). The function $\mathcal{V}(\theta^2, z, \epsilon)$ in Eq. (5.1) then reads

$$\mathcal{V}(\theta^2, z, \epsilon) = \mathcal{V}_{\text{renorm.}}(\theta^2, z, \epsilon) + \mathcal{V}_{g \rightarrow q\bar{q}}^{(1)}(\theta^2, z, \epsilon) + \mathcal{V}_{g \rightarrow gg}^{(1)}(\theta^2, z, \epsilon) + \mathcal{V}_{H \rightarrow gg}^{(1)\text{Born}}(\theta^2, z, \epsilon). \quad (5.12)$$

6 Real $1 \rightarrow 3$ collinear splitting

In this section we discuss the integration of the triple-collinear splitting functions over the three-body phase space, while keeping fixed z and θ as discussed in Sec. 4. We start by introducing the spin-averaged triple-collinear splitting functions relevant for gluon fragmentation. By considering the spin-averaged case, we implicitly focus on observables that are insensitive to spin correlations. For an initial gluon there are three distinct splitting functions to consider organised by colour structure. In the notation of Ref. [63] these are:

- $\langle \hat{P}_{g_1 g_2 g_3} \rangle$ corresponding to a $1 \rightarrow 3$ gluon splitting into three gluons.
- $\langle \hat{P}_{g_1 q_2 \bar{q}_3}^{(\text{ab})} \rangle$ corresponding to the abelian channel, $C_F T_R n_f$, of a gluon splitting into a $q\bar{q}$ pair, with subsequent emission of a gluon.
- $\langle \hat{P}_{g_1 q_2 \bar{q}_3}^{(\text{nab})} \rangle$ corresponding to the non-abelian channel, $C_A T_R n_f$, of a gluon splitting into two gluons, one of which branches further into a $q\bar{q}$ pair.

The splitting functions in Ref. [63] are expressed in terms of invariants, s_{ij} , and energy fractions z_i . In the relevant collinear limit, we have that $s_{ij} = (p_i + p_j)^2 \simeq E^2 z_i z_j \theta_{ij}^2$ where E denotes the energy of the initial gluon. The triple-collinear phase space in $d = 4 - 2\epsilon$ dimensions may be expressed in the form [72]

$$d\Phi_3 = \frac{1}{\pi} \frac{E^{4-4\epsilon}}{(4\pi)^{4-2\epsilon} \Gamma(1-2\epsilon)} dz_2 dz_3 d\theta_{13}^2 d\theta_{23}^2 d\theta_{12}^2 (z_1 z_2 z_3)^{1-2\epsilon} \Delta^{-1/2-\epsilon} \Theta(\Delta) , \quad (6.1)$$

where the Gram determinant is given by

$$\Delta = 4\theta_{ik}^2 \theta_{jk}^2 - (\theta_{ij}^2 - \theta_{ik}^2 - \theta_{jk}^2)^2, \quad i \neq j \neq k , \quad (6.2)$$

and

$$\sum_{i=1}^3 z_i = 1. \quad (6.3)$$

As explained before, we are interested in the double-differential distribution in (z, θ) , which is defined according to the procedure of Sec. 4 and will be illustrated in the following:

- $C_{ATR} n_f$: This colour channel exhibits a simple collinear structure because the sole collinear singularity appears as $\theta_{23} \rightarrow 0$, see Fig. 1. Therefore, we fix the energy fraction of the gluon to be $z_1 = z$ and the angle $\theta = \theta_g$ shown in Fig. 1. We map the set (z_1, z_2, z_3) into an independent set (z, z_p) defined as shown in the figure. Instead when z falls below z_{cut} , the angle will be defined as $\theta = \theta_{23}$ and the longitudinal momentum defined as $z = z_2$ as shown in Fig. 2.

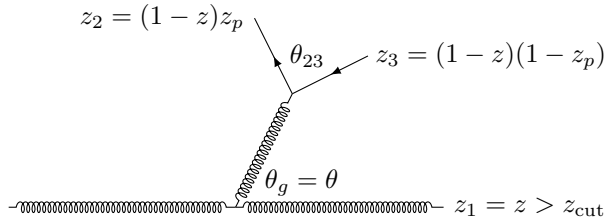


Figure 1: The Feynman diagram representing gluon emission followed by its subsequent decay to a $q\bar{q}$ pair.

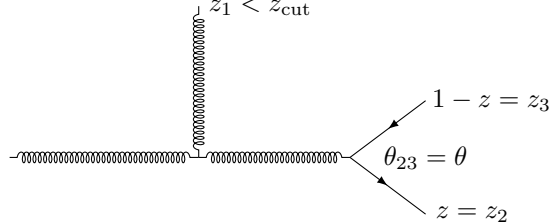


Figure 2: The Feynman diagram representing gluon emission followed by its subsequent decay to a $q\bar{q}$ pair, where g_1 goes below the energy threshold and is allowed to fly off at wide angles.

- $C_{FTR} n_f$: This colour channel exhibits two collinear singularities as $\theta_{13} \rightarrow 0$ and $\theta_{12} \rightarrow 0$, see Fig. 3. Therefore, we partition the phase space into two sectors $\theta_{13} < \theta_{12}$ and $\theta_{12} < \theta_{13}$. In the former, we fix the quark energy $z_2 = 1 - z$ and the angle $\theta = \theta_{2,13}$. In the latter we fix the anti-quark energy $z_3 = z$ and the angle $\theta = \theta_{3,12}$. The configurations in which $z < z_{cut}$ ($z > 1 - z_{cut}$) in sector 1 (2) correspond to power-suppressed contributions in z_{cut} (due to a soft quark) and are therefore neglected.
- C_A^2 : This channel is the most complicated since there is a collinear pole as any angle $\theta_{ij} \rightarrow 0$. Therefore, we partition the phase space into three distinct sectors defined

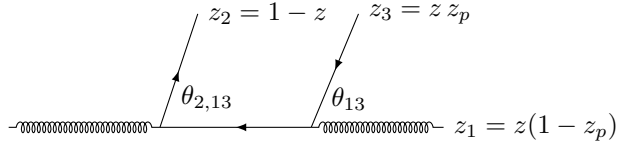


Figure 3: The Feynman diagram representing the $q\bar{q}$ emission, and the energy fraction parameterisation is suitable for the region $\theta_{13} < \theta_{12}$.

by the smallest angle in each. For example, in the sector $\min\{\theta_{ij}\} = \theta_{12}$ we fix the angle between the parent of the clustered pair and the remaining gluon, i.e. $\theta = \theta_{12,3}$ as shown in Fig. 4. The above sectoring removes a 1/3 combinatorial factor, and in order to remove the remaining twofold symmetry in the $g \rightarrow ggg$ splitting function we require that $z_p \geq 1/2$ in the parameterisation of Fig. 4.¹¹ The energy fraction being fixed is $z_3 = z$. When z falls below z_{cut} , then $\theta = \theta_{12}$ and $z = z_2$.

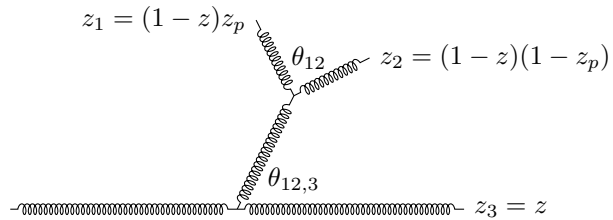


Figure 4: The Feynman diagram representing gluon emission followed by its subsequent decay to a gg pair, where the energy fraction parameterisation suitable for the angular region $\min\{\theta_{ij}\} = \theta_{12}$ is shown.

We integrate the splitting functions over the three-body phase space in $d = 4 - 2\epsilon$ dimensions to obtain real emission contributions. The integrals we carry out are generically of the form

$$\frac{\theta^2}{\sigma_0} \frac{d^2\sigma}{dz d\theta^2} = \int d\Phi_3(z_i, \theta_{ij}) \frac{(8\pi\alpha_s \mu^{2\epsilon})^2}{s_{123}^2} \langle \hat{P} \rangle \theta^2 \delta(\theta^2 - \theta^2(z_i, \theta_{ij})) \delta(z - z(z_i)) \Theta_{\text{cut}}(\theta_{ij}), \quad (6.4)$$

where $\Theta_{\text{cut}}(\theta_{ij})$ denotes the angular cuts due to sectoring that we described above. We evaluate the above integrals by expanding out the singular structure as a Laurent series in distributions, and then handle the remaining integrations with **Mathematica**.

6.1 The $C_{FT_R} n_f$ channel

We start with the $C_{FT_R} n_f$ channel. The splitting function to be integrated is the unpolarised quantity $\langle \hat{P}_{g_1 q_2 \bar{q}_3} \rangle$ from Ref. [63]. The approach to the calculation of the corresponding phase-space integrals, as well as other computational details, are discussed in the corresponding calculation for the quark fragmentation given in Refs. [57, 66].

¹¹We observe that any choice of the angle that is kept fixed to θ which is equivalent in the singular limits will produce the same result for $\mathcal{B}_2^g(z)$, e.g. one could also choose to fix $\theta = \theta_{13}$, and would only differ by further subleading (N^3LL) corrections.

Following our definition of z and θ , we consider two sectors: $\theta_{13} < \theta_{12}$, which contains the collinear singularity along the antiquark, and $\theta_{12} < \theta_{13}$, which contains the collinear singularity along the quark. In the first sector we parameterise the momenta as if the gluon is emitted from the antiquark so that $z_2 = (1 - z)$, $z_3 = zz_p$ and $z_1 = z(1 - z_p)$ as shown in Fig. 3. In the second sector we instead parameterise the energy fractions as if the gluon is emitted from the quark, i.e. $z_3 = z$, $z_1 = (1 - z_p)(1 - z)$ and $z_2 = z_p(1 - z)$. We also fix the angle $\theta \equiv \theta_{2,13}$ in the first sector, and $\theta \equiv \theta_{3,12}$ in the second sector. We can just perform the calculation in the first sector and obtain the answer in the second sector by sending $z \rightarrow 1 - z$. We report below the real emission contribution for the sector $\theta_{13} < \theta_{12}$ which can be expressed as:

$$\left(\frac{\theta^2}{\sigma_0} \frac{d^2 \sigma_{\mathcal{R}}^{(2)}}{d\theta^2 dz} \right)^{C_F T_R n_f, \text{sec.1}} = C_F T_R n_f \left(\frac{\alpha_s}{2\pi} \right)^2 \left(\frac{H_{\text{soft-coll.}}^{\text{sec.1}}(\theta^2, z, \epsilon)}{\epsilon^2} + \frac{H_{\text{coll.}}^{\text{sec.1}}(\theta^2, z, \epsilon)}{\epsilon} \right. \\ \left. + \frac{H_{\text{soft}}^{\text{sec.1}}(\theta^2, z, \epsilon)}{\epsilon} + H_{\text{fin.}}^{\text{sec.1}}(z) \right), \quad (6.5)$$

where the functions are labeled according to the origin of the singular behaviour and $H_{\text{fin.}}^{\text{sec.1}}(z)$ is a finite function that we cast as a 1-fold integral over z_p . As the gluon is emitted from the (anti)-quark, the singular structure is identical to that for the C_F^2 quark jet case, and reported in Refs. [57, 66], *viz.*

$$H_{\text{soft-coll.}}^{\text{sec.1}}(\theta^2, z, \epsilon) = z^{-4\epsilon} (1 - z)^{-2\epsilon} \theta^{-4\epsilon} p_{qg}(z, \epsilon) \left(1 - \frac{\pi^2}{6} \epsilon^2 + \mathcal{O}(\epsilon^3) \right), \\ H_{\text{coll.}}^{\text{sec.1}}(\theta^2, z, \epsilon) = z^{-4\epsilon} (1 - z)^{-2\epsilon} \theta^{-4\epsilon} p_{qg}(z, \epsilon) \left(\frac{3}{2} + \frac{13}{2} \epsilon - \frac{2\pi^2}{3} \epsilon + \mathcal{O}(\epsilon^2) \right), \\ H_{\text{soft}}^{\text{sec.1}}(\theta^2, z, \epsilon) = 0.$$
(6.6)

The result in the second sector can be obtained quite easily from the first by sending $z \rightarrow 1 - z$. In particular,

$$H_{\text{fin.}}^{\text{sec.2}}(z) = H_{\text{fin.}}^{\text{sec.1}}(1 - z). \quad (6.7)$$

We plot the total finite function, $H_{\text{fin.}}^{C_F T_R} \equiv H_{\text{fin.}}^{\text{sec.1}} + H_{\text{fin.}}^{\text{sec.2}}$ in Fig. 5. The divergent behavior of $H_{\text{fin.}}^{C_F T_R}(z)$ as $z \rightarrow 0$ or $z \rightarrow 1$ is only logarithmic, and thus it is integrable over $z \in [0, 1]$. The integral read

$$\int_0^1 dz H_{\text{fin.}}^{C_F T_R}(z) = -3. \quad (6.8)$$

6.2 The $C_A T_R n_f$ channel

We start with the configuration depicted in Fig. 1. For this channel channel, a convenient parametrisation of the three body phase space can be obtained in terms of web variables as discussed in Ref. [57]. The only collinear singularity in this channel emerges from the collinear $g \rightarrow q\bar{q}$ splitting, i.e. when $\theta_{23} \rightarrow 0$. Therefore, following our procedure outlined in

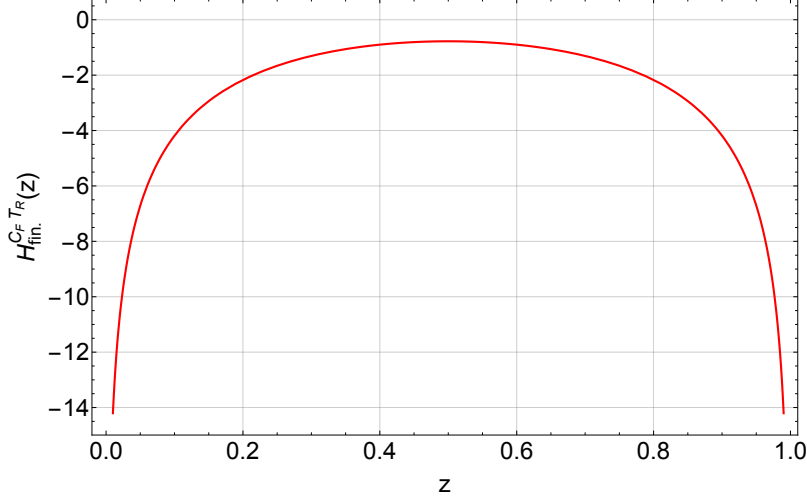


Figure 5: The function $H_{\text{fin.}}^{CFT_R}(z)$.

Sec. 4, there is a single sector and thus we can integrate inclusively over the angular phase space. In this channel we need to consider the two situations depicted in Figs. 1 and 2, in which the branching with a larger angle either passes or does not pass the z_{cut} threshold. In the first case, the longitudinal momentum kept fixed is $z_1 = z$ (with $1 - z_{\text{cut}} > z > z_{\text{cut}}$). We fix the angle θ to be that of the parent of the (23) pair, $\theta = \theta_{23,1} = \theta_g$, which reads

$$\theta_g^2 = \frac{z_2}{z_2 + z_3} \theta_{12}^2 + \frac{z_3}{z_2 + z_3} \theta_{13}^2 - \frac{z_2 z_3}{(z_2 + z_3)^2} \theta_{23}^2 . \quad (6.9)$$

Finally, we symmetrise in $z \leftrightarrow 1 - z$ and multiply by $1/2!$ to obtain:

$$\begin{aligned} \left(\frac{\theta^2}{\sigma_0} \frac{d^2 \sigma_{\mathcal{R}}^{(2)}}{d\theta^2 dz} \right)_{z_1 > z_{\text{cut}}}^{C_A T_R} &= \frac{1}{2!} C_A T_R n_f \left(\frac{\alpha_s}{2\pi} \right)^2 z^{-3\epsilon} (1-z)^{-3\epsilon} \theta^{-4\epsilon} \left[p_{gg}(z) \left(-\frac{8}{3\epsilon} - \frac{40}{9} \right) \right. \\ &\quad \left. - \frac{4}{3} (1+z) \ln z - \frac{4}{3} (2-z) \ln(1-z) + \frac{26}{9} \left(z^2 + (1-z)^2 - \frac{1}{z(1-z)} \right) + \frac{10}{3} \right] \\ &\quad \times \Theta(z - z_{\text{cut}}) \Theta(1 - z_{\text{cut}} - z) . \end{aligned} \quad (6.10)$$

In the second case (see Fig. 2), the first gluon fails the z_{cut} condition. Accordingly, z and θ are now fixed by the kinematics of the hard $g \rightarrow q\bar{q}$ splitting. We note that, in contrast to the $CFT_R n_f$ channel, the failure of the z_{cut} condition is now associated with a soft gluon divergence. In the $z_1 \rightarrow 0$ soft limit, the spin averaged splitting kernel factorises into a product of an eikonal factor (associated to the emission of g_1) and a $1 \rightarrow 2$ splitting function. In this configuration we obtain:

$$\begin{aligned} \left(\frac{\theta^2}{\sigma_0} \frac{d^2 \sigma_{\mathcal{R}}^{(2)}}{d\theta^2 dz} \right)_{z_1 < z_{\text{cut}}}^{C_A T_R} &= \left(\frac{\alpha_s}{2\pi} \right)^2 C_A T_R n_f (2z(1-z))^{-2\epsilon} \theta^{-2\epsilon} p_{gg}(z, \epsilon) \times \\ &\quad \times \left(-\frac{z_{\text{cut}}^{-2\epsilon}}{\epsilon} \ln \frac{4}{\theta^2} - \frac{\pi^2}{6} - \frac{1}{2} \ln^2 \frac{4}{\theta^2} \right) \Theta(z - z_{\text{cut}}) \Theta(1 - z_{\text{cut}} - z) . \end{aligned} \quad (6.11)$$

This result is similar to what was obtained for quark jets in the C_F^2 channel reported in Eq. (27) of Ref. [66], modulo the replacement $p_{qq} \rightarrow p_{qg}$. The final result is obtained as the sum of the two contributions Eqs. (6.10) and (6.11).

6.3 The C_A^2 channel

As explained in Sec. 4, we work in the region $\min\{\theta_{ij}\} = \theta_{12}$, see Fig. 4. This is completely general as the other sectors have an identical structure due to the three-fold symmetry present in the splitting kernel. To account for the full $1/3!$ symmetry factor, one can simply choose $z_p < 1 - z_p$. Clearly in this sector the only collinear singularity arises when $\theta_{12} \rightarrow 0$. As in the $C_A T_R n_f$ channel, also in this case we have to consider two scenarios, i.e. when the gluon at larger angle either passes or fails the z_{cut} condition. In the first scenario, the angular variable to be fixed is $\theta = \theta_{12,3} = \theta_g$ now defined as

$$\theta_g^2 = \frac{z_1}{z_1 + z_2} \theta_{13}^2 + \frac{z_2}{z_1 + z_2} \theta_{23}^2 - \frac{z_1 z_2}{(z_1 + z_2)^2} \theta_{12}^2 , \quad (6.12)$$

and $z_3 = z$ (with $1 - z_{\text{cut}} > z > z_{\text{cut}}$). We obtain:

$$\left(\frac{\theta^2}{\sigma_0} \frac{d^2 \sigma_{\mathcal{R}}^{(2)}}{d\theta^2 dz} \right)_{z_3 > z_{\text{cut}}}^{C_A^2} = C_A^2 \left(\frac{\alpha_s}{2\pi} \right)^2 \left(\frac{H_{\text{soft-coll.}}(\theta^2, z, \epsilon)}{\epsilon^2} + \frac{H_{\text{coll.}}(\theta^2, z, \epsilon)}{\epsilon} \right. \\ \left. + \frac{H_{\text{soft}}(\theta^2, z, \epsilon)}{\epsilon} + H_{\text{fin.}}^{C_A^2}(z) \right) \Theta(z - z_{\text{cut}}) \Theta(1 - z_{\text{cut}} - z) , \quad (6.13)$$

where we have symmetrised over $z \leftrightarrow 1 - z$. The functions appearing in the above equation are given by

$$H_{\text{soft-coll.}}(\theta^2, z, \epsilon) = z^{-2\epsilon} (1 - z)^{-2\epsilon} (z^{-2\epsilon} + (1 - z)^{-2\epsilon}) \theta^{-4\epsilon} 4^{2\epsilon} p_{gg}(z) \left(1 - \frac{\pi^2}{6} \epsilon^2 \right) , \\ H_{\text{coll.}}(\theta^2, z, \epsilon) = -z^{-2\epsilon} (1 - z)^{-2\epsilon} (z^{-2\epsilon} + (1 - z)^{-2\epsilon}) \theta^{-4\epsilon} 4^\epsilon p_{gg}(z) \\ \times \left(-\frac{11}{6} + 2 \ln 2 + \epsilon \left(-\frac{67}{9} + \frac{2\pi^2}{3} + 2 \ln^2 2 \right) \right) , \\ H_{\text{soft}}(\theta^2, z, \epsilon) = -z^{-2\epsilon} (1 - z)^{-2\epsilon} (z^{-2\epsilon} + (1 - z)^{-2\epsilon}) \theta^{-4\epsilon} 4^\epsilon p_{gg}(z) \left(2 \ln 2 + h_{\text{pass}}^{\text{poles}} \epsilon \right) , \quad (6.14)$$

where $h_{\text{pass}}^{\text{poles}}$ is a numerical constant that reads

$$h_{\text{pass}}^{\text{poles}} \simeq 1.32644693(2) . \quad (6.15)$$

The uncertainty in the above number is on the last quoted digit, which has been rounded as indicated by the bracket notation. We will use the same notation for all numerical constants quoted in the following, unless an error is explicitly quoted. As expected from the structure of the gluon splitting functions, the function $H_{\text{fin.}}^{C_A^2}(z)$ has soft divergences as $z \rightarrow 0$ and $z \rightarrow 1$ which can be singled out, leading to

$$H_{\text{fin.}}^{C_A^2}(z) = -\frac{h_{\text{pass}}^{\text{fin}}}{z(1 - z)} + G_{z_3 > z_{\text{cut}}}(z) . \quad (6.16)$$

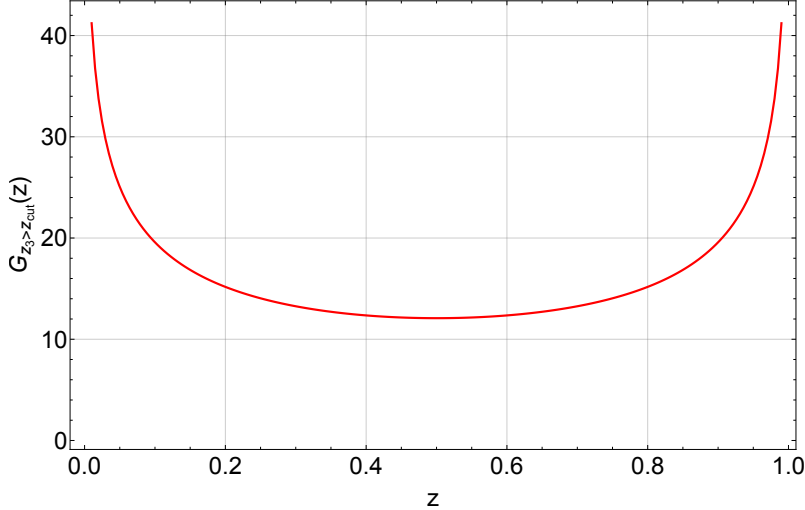


Figure 6: The function $G_{z_3 > z_{\text{cut}}}(z)$.

The coefficient of the soft divergences at $z = 1$ and $z = 0$ in the above expression is the result of a two-fold integration which can be performed with very high numerical precision. We obtain

$$h_{\text{pass}}^{\text{fin}} \simeq 3.31674336(8). \quad (6.17)$$

The quantity $G_{z_3 > z_{\text{cut}}}(z)$ is fully regular and can be integrated over $z \in [0, 1]$

$$\int_0^1 dz G_{z_3 > z_{\text{cut}}}(z) \simeq 16.947 \pm 0.004. \quad (6.18)$$

The function $G_{z_3 > z_{\text{cut}}}(z)$ for this colour channel is displayed in Fig. 6. The decomposition in Eq. (6.16) will be important later in the extraction of the NNLL hard collinear coefficient $\mathcal{B}_2^g(z)$, which requires a consistent subtraction of the soft contributions.

We now consider the second scenario in which $z_3 < z_{\text{cut}}$. In the C_A^2 channel, this contribution contains a physical difference from the corresponding result quoted in Eq. (6.11). The difference comes from the fact that in the $z_3 \rightarrow 0$ limit, the matrix element does not factorise into the product of independent emissions matrix elements, except for the limit in which the gluon pair that passes the cut is well separated in angle from the gluon that fails the cut, i.e. with the notation of Fig. 4, $\theta_{13} \sim \theta_{23} \gg \theta_{12}$. We can then organise the result as the sum of a term analogous to Eq. (6.11), given below

$$\left(\frac{\theta^2}{\sigma_0} \frac{d^2 \sigma_{\mathcal{R}}^{(2)}}{d\theta^2 dz} \right)_{z_3 < z_{\text{cut}}}^{C_A^2, (A)} = \left(\frac{\alpha_s}{2\pi} \right)^2 C_A^2 (2z(1-z))^{-2\epsilon} \theta^{-2\epsilon} p_{gg}(z) \times \\ \times \left(-\frac{z_{\text{cut}}^{-2\epsilon}}{\epsilon} \ln \frac{4}{\theta^2} - \frac{\pi^2}{6} - \frac{1}{2} \ln^2 \frac{4}{\theta^2} \right) \Theta(z - z_{\text{cut}}) \Theta(1 - z_{\text{cut}} - z), \quad (6.19)$$

and a new contribution stemming from the non-independent (i.e. correlated) emission con-

tribution. This is evaluated numerically and obtain

$$\left(\frac{\theta^2}{\sigma_0} \frac{d^2 \sigma_{\mathcal{R}}^{(2)}}{d\theta^2 dz} \right)_{z_3 < z_{\text{cut}}}^{C_A^2, (B)} = h_{\text{fail}}^{p_{gg}} p_{gg}(z) \Theta(z - z_{\text{cut}}) \Theta(1 - z_{\text{cut}} - z) + h_{\text{fail}}^{\delta} \delta(z), \quad (6.20)$$

where

$$h_{\text{fail}}^{p_{gg}} \simeq 0.731081807(5), \quad h_{\text{fail}}^{\delta} \simeq -8.42858916(9). \quad (6.21)$$

7 Extraction of $\mathcal{B}_2^g(z)$

Now we use the results obtained in the previous two sections to extract the function $\mathcal{B}_2^g(z)$. As we stressed before $\mathcal{B}_2^g(z)$ reflects the NNLL dynamics that does not arise from strongly-ordered physics. We follow the procedure outlined in Sec. 4 to extract $\mathcal{B}_2^g(z)$, and after adding real and virtual corrections for each colour channel we need to remove pieces pertaining to NLL physics. In analogy with Eq. (2.10) for quark jets we write down our defining equation for $\mathcal{B}_2^g(z)$ starting from the NNLL evolution equation for $G_g(x, t)$

$$G_g(x, t) = u \Delta_g(t) + \int_t^{t_0} dt' \int_{z_0}^{1-z_0} dz \left[\mathcal{P}_{gg}(z, \theta) G_g(x z, t') G_g(x(1-z), t') \right. \\ \left. + \mathcal{P}_{qg}(z, \theta) G_q(x z, t') G_q(x(1-z), t') \right] \frac{\Delta_g(t)}{\Delta_g(t')} + \mathbb{K}_g^{\text{finite}}[G_q, G_g], \quad (7.1)$$

where $\mathbb{K}_g^{\text{finite}}[G_q, G_g]$ is given in Appendix C and the inclusive emission probabilities for gluon jets are given by

$$\mathcal{P}_{gg}(z, \theta) \equiv \frac{C_A}{1-z} \left(1 + \frac{\alpha_s(E^2(1-z)^2\theta^2)}{2\pi} K^{(1)} \right) \\ + \frac{\alpha_s(E^2z^2\theta^2)}{\alpha_s(E^2(1-z)^2\theta^2)} \frac{C_A}{z} \left(1 + \frac{\alpha_s(E^2z^2\theta^2)}{2\pi} K^{(1)} \right) \\ + \mathcal{B}_1^{gg}(z) + \frac{\alpha_s(E^2(1-z)^2\theta^2)}{2\pi} (\mathcal{B}_2^{gg}(z) + \mathcal{B}_1^{gg}(z) b_0 \ln(1-z)^2), \\ \mathcal{P}_{qg}(z, \theta) \equiv \mathcal{B}_1^{qg}(z) + \frac{\alpha_s(E^2(1-z)^2\theta^2)}{2\pi} (\mathcal{B}_2^{qg}(z) + \mathcal{B}_1^{qg}(z) b_0 \ln(1-z)^2), \quad (7.2)$$

where the LO anomalous dimensions read

$$\mathcal{B}_1^{gg}(z) = C_A (z(1-z) - 2), \quad \mathcal{B}_1^{qg}(z) = T_R n_f (z^2 + (1-z)^2). \quad (7.3)$$

The ratio of strong couplings in the second line of $\mathcal{P}_{gg}(z, \theta)$ has the role of restoring the correct scale of the coupling corresponding to the soft singularity as $z \rightarrow 0$ as opposed to the one at $z \rightarrow 1$ that is encoded in the evolution time (2.1). This feature is of course present exclusively for gluon jets, and it is absent in the quark case (2.10). The quantity $\mathcal{B}_2^g(z)$ is then simply the sum of $\mathcal{B}_2^{gg}(z)$ and $\mathcal{B}_2^{qg}(z)$. A subtle aspect of the above decomposition between terms that are interpreted as corrections to either the $g \rightarrow gg$ or the $g \rightarrow q\bar{q}$ channel is that they both receive a contribution from the $C_A T_R$ colour factor. The separation between such contributions to $\mathcal{B}_2^g(z)$ is not unique and the ambiguity is

immaterial as one can decide to assign the whole correction to either of the two flavour channels. Conventionally we include it as a correction to $g \rightarrow gg$. We thus write:

$$\begin{aligned}\mathcal{B}_2^{gg}(z) &\equiv C_A T_R n_f \mathcal{B}_2^{g, C_A T_R}(z) + C_A^2 \mathcal{B}_2^{g, C_A^2}(z), \\ \mathcal{B}_2^{gg}(z) &\equiv T_R^2 n_f^2 \mathcal{B}_2^{g, T_R^2}(z) + C_F T_R n_f \mathcal{B}_2^{g, C_F T_R}(z).\end{aligned}\quad (7.4)$$

The Sudakov form factor for gluon jets, given at NLL in Eq. (2.5), at NNLL then reads

$$\ln \Delta_g(t) = - \int_t^{t_0} dt' \int_{z_0}^{1-z_0} dz (\mathcal{P}_{gg}(z, \theta) + \mathcal{P}_{qg}(z, \theta)). \quad (7.5)$$

In the following we carry out the calculation of $\mathcal{B}_2^g(z)$ in each of the above colour channels.

7.1 The $T_R^2 n_f^2$ channel

This channel is distinct in that it has no double real contribution. From Eqs. (5.4), (5.5), (5.11) and after subtracting the NLL contribution that emerges from Eq. (D.13) we obtain

$$\mathcal{B}_2^{g, T_R^2}(z) = p_{qg}(z) \left(\frac{1}{3} + \frac{4}{3} \ln(z(1-z)) \right), \quad (7.6)$$

which integrates to

$$\int_0^1 dz \mathcal{B}_2^{g, T_R^2}(z) = -\frac{46}{27}. \quad (7.7)$$

7.2 The $C_F T_R n_f$ channel

The extraction of $\mathcal{B}_2^g(z)$ in this channel is very simple since it starts at NNLL and hence there is no need to subtract NLL contributions from the total result. Thus we add real, Eq. (6.5) and its mirror symmetric obtained by the swap $z \leftrightarrow 1-z$, and virtual, Eq. (5.5), corrections to find

$$\mathcal{B}_2^{g, C_F T_R}(z) = p_{qg}(z) \left(\ln^2 \left(\frac{z}{1-z} \right) - \frac{\pi^2}{3} + 5 \right) + H_{\text{fin.}}^{C_F T_R}(z), \quad (7.8)$$

whose integral reads

$$\int_0^1 dz \mathcal{B}_2^{g, C_F T_R}(z) = 1. \quad (7.9)$$

7.3 The $C_A T_R n_f$ channel

We combine the real and virtual terms Eqs. (6.10), (6.11), (5.4), (5.5), (5.9) and (5.11) and then subtract the NLL contribution that emerges from Eq. (D.13), to obtain

$$\begin{aligned}\mathcal{B}_2^{g, C_A T_R}(z) &= -p_{qg}(z) (\ln^2 z + \ln^2(1-z)) + \frac{1}{9}(28 - 41z + 41z^2) \\ &+ \ln z \left(\frac{4}{3(1-z)} - \frac{26}{3}z^2 + 8z - 7 \right) + \ln(1-z) \left(\frac{4}{3z} - \frac{26}{3}(1-z)^2 + 8(1-z) - 7 \right),\end{aligned}\quad (7.10)$$

which integrates to

$$\int_0^1 dz \mathcal{B}_2^{g,C_A T_R}(z) = \frac{593}{54} - \frac{4\pi^2}{9}. \quad (7.11)$$

Before we discuss the more involved C_A^2 channel, it is instructive to compare the integral of the contributions to $\mathcal{B}_2^g(z)$ computed so far to the expectation given in Eq. (4.2). In particular, given that the term $\mathcal{F}_{\text{clust.}}^{C_A^2}$ is a pure C_A^2 contribution, the combination of Eqs. (7.7), (7.11) allows us to extract the constant $X_{\theta^2}^g$ corresponding to the observable $\frac{\theta^2}{\sigma_0} \frac{d^2\sigma}{d\theta^2 dz}$ used in the calculation. This yields

$$X_{\theta^2}^g = -C_A \left(\frac{67}{9} - \frac{2\pi^2}{3} \right) + \frac{23}{9} T_R n_f, \quad (7.12)$$

which can be used as a cross check in the C_A^2 channel below.

7.4 The C_A^2 channel

The procedure for extracting $\mathcal{B}_2(z)$ is the same as in the previous channel. The relevant real emission terms are given in Eqs. (6.13), (6.19), (6.20) which can then be combined with the virtual contributions emerging from Eqs. (5.4), (5.9), (5.11). After removal of NLL terms the result can be expressed as

$$\mathcal{B}_2^{g,C_A^2}(z) = \mathcal{B}_2^{g,C_A^2,\text{analytic}}(z) + G_{z_3 > z_{\text{cut}}}(z) + \mathcal{B}_2^{\text{endpoint}}(z). \quad (7.13)$$

The term $\mathcal{B}_2^{g,C_A^2,\text{analytic}}(z)$ is computed analytically while the contribution $G_{z_3 > z_{\text{cut}}}(z)$ is determined numerically. Finally there is an endpoint contribution which originates purely from the double-soft limit. This includes the clustering correction as well as the numerically computed contributions from the region where $z_3 < z_{\text{cut}}$. The term $\mathcal{B}_2^{g,C_A^2,\text{analytic}}(z)$ reads:

$$\begin{aligned} \mathcal{B}_2^{g,C_A^2,\text{analytic}}(z) &= p_{gg}(z) \left(-2 \ln z \ln(1-z) - \frac{11}{3} \ln z - \frac{11}{3} \ln(1-z) \right) \\ &+ \frac{11}{3} \left(\frac{\ln z}{z} + \frac{\ln(1-z)}{1-z} \right) - \frac{265}{18} + \frac{\pi^2}{3} (2 - z(1-z)) + 4 h_{\text{pass}}^{\text{poles}} - \frac{44}{3} \ln 2 + 8 \ln^2 2 \\ &- 2z(1-z) \left(-\frac{67}{18} + h_{\text{pass}}^{\text{poles}} + 2 \ln^2 2 - \frac{11}{3} \ln 2 \right) + h_{\text{fail}}^{p_{gg}} (-2 + z(1-z)). \end{aligned} \quad (7.14)$$

Its integral is straightforward and gives:

$$\int dz \mathcal{B}_2^{g,C_A^2,\text{analytic}}(z) = -\frac{535}{27} + \frac{11\pi^2}{9} + \frac{11}{3} h_{\text{pass}}^{\text{poles}} - \frac{121}{9} \ln 2 + \frac{22}{3} \ln^2 2 - 4\zeta(3) - \frac{11}{6} h_{\text{fail}}^{p_{gg}}. \quad (7.15)$$

The end-point contribution is simply given by

$$\mathcal{B}_2^{\text{endpoint}}(z) = h_{\text{fail}}^\delta \delta(z). \quad (7.16)$$

The constants $h_{\text{pass}}^{\text{poles}}$, $h_{\text{fail}}^{p_{gg}}$, and h_{fail}^δ are defined in Eqs. (6.15), (6.21) and the function $G_{z_3 > z_{\text{cut}}}(z)$ is defined in Eq. (6.16). The total integral of $\mathcal{B}_2^{g,C_A^2}(z)$ then yields

$$\int_0^1 dz \mathcal{B}_2^{g,C_A^2}(z) \simeq -6.314 \pm 0.004. \quad (7.17)$$

As a cross check of the above result we can compare to the expected integral in Eq. (4.2), where $X_{\theta^2}^g$ is given in Eq. (7.12). For this check we still have to determine the function $\mathcal{F}_{\text{clust.}}^{C_A^2}$. For the C_A^2 channel our procedure for the extraction of $\mathcal{B}_2^{g,C_A^2}(z)$ agrees exactly with the mMDT/Soft drop grooming with the Cambridge/Aachen algorithm, for which $\mathcal{F}_{\text{clust.}}^{C_A^2}$ is known to stem from the double-soft limit (within the triple-collinear approximation). Therefore, due to Casimir scaling it is simple to relate the clustering correction $\mathcal{F}_{\text{clust.}}^{C_A^2}$ to the known result for quark jets (see e.g. [66]) (cf. also the discussion in Appendix E). Replacing $C_F \rightarrow C_A$ in the quark jet result we get the following result the C_A^2 component reads:

$$\mathcal{F}_{\text{clust.}}^{C_A^2} = \frac{1}{2} C_A^2 \left(\frac{4\pi}{3} \text{Cl}_2 \left(\frac{\pi}{3} \right) + h_{\text{clust.}}^{C_A} \right), \quad (7.18)$$

where

$$h_{\text{clust.}}^{C_A} \simeq -1.16363257(4), \quad (7.19)$$

and Cl_2 denotes the Clausen function. The overall factor of $1/2$ is multiplied to obtain the result for a single leg. This gives

$$(-\gamma_g^{(2)} + b_0 X_{\theta^2}^g + \mathcal{F}_{\text{clust.}})_{C_A^2} \simeq -6.31426325(8) C_A^2, \quad (7.20)$$

in good agreement with our result.

We conclude this section with a remark on the endpoint contribution $\mathcal{B}_2^{\text{endpoint}}(z)$ given in Eq. (7.16). As discussed above, this originates from double-soft configurations and is a consequence of the scheme used here to define z and θ . We observe that such endpoint terms mark an important difference to the case of quark jets (cf. Appendix B), where separate definitions of z and θ can be adopted for correlated and independent emission contributions. In the quark case these are separated by colour factors, while in the gluon case they are mixed together in the C_A^2 channel. The same double-soft origin is shared by the clustering correction (7.18). Terms of double-soft origin are discussed further in Appendix E.

8 Moments of EEC and angularities in groomed jets at NNLL

In this section we use the calculations presented in this article to derive NNLL results for the moments of energy-energy correlation (EEC) and angularities measured on jets groomed according to the mMDT/Soft drop ($\beta = 0$) procedure [60, 61]. These classes of jet substructure observables have received widespread attention in the literature, with several applications both at hadron and lepton colliders [73–86]. As a concrete example we consider the processes $Z \rightarrow q\bar{q}$ and $H \rightarrow gg$ to analyse both quark and gluon jets. Specifically, we calculate, for the first time, the groomed fractional moments of EEC, which are defined as [58]

$$FC_x^{\mathcal{H}} = \frac{2^{-x}}{E^2} \sum_{i \neq j} E_i E_j |\sin \theta_{ij}|^x (1 - |\cos \theta_{ij}|)^{1-x}, \quad (8.1)$$

where the sum runs over all particles within a given hemisphere, $\mathcal{H} \equiv \mathcal{H}_R$ or $\mathcal{H} \equiv \mathcal{H}_L$, and E denotes the total energy in the hemisphere. We also consider the angularities [59] (the corresponding NNLL resummation in the ungroomed case is given in Refs. [55, 87–90]) defined w.r.t. the Winner-Take-All (WTA) axis as

$$\lambda_x^{\mathcal{H}} = \frac{2^{1-x}}{E} \sum_i E_i |\sin \theta_i|^x (1 - |\cos \theta_i|)^{1-x}, \quad (8.2)$$

where once again the sum involves all particles in a given hemisphere. For both observables the parameter x is constrained by IR safety to be $x < 2$. Finally, we define the observables as follows:

$$FC_x \equiv \max \{FC_x^{\mathcal{H}_R}, FC_x^{\mathcal{H}_L}\}, \lambda_x \equiv \max \{\lambda_x^{\mathcal{H}_R}, \lambda_x^{\mathcal{H}_L}\}. \quad (8.3)$$

A NNLL calculation for WTA angularities for quark jets has been recently presented in Ref. [67],¹² and below we present new results for fractional moments of EEC for quark and gluon jets as well as for angularities measured on gluon jets. These results allow for a complete phenomenological analysis of moments of EEC and angularities on groomed jets at hadron and lepton colliders.

The master formula for the NNLL cumulative cross section $\Sigma(v)$ for a groomed observable v (that here denotes either a moment of EEC or an angularity) in the two processes considered here can be easily derived by applying the GFs method to Eq. (2.7). In the following we work in the limit $v \ll z_{\text{cut}} \ll 1$, that is commonly considered for these types of groomed observables. This regime has the advantage that one can neglect power corrections in z_{cut} and hence the evolution equations for the GFs can be solved analytically. Specifically, in this limit we can restrict ourselves to taking the *soft limit* of the $\mathbb{K}_q^{\text{finite}}[G_q, G_g]$ and $\mathbb{K}_g^{\text{finite}}[G_q, G_g]$ functions (cf. Eqs. (2.9), (7.1) and Appendix C). With a little abuse of notation we have used the same parameter z_{cut} for the definition of groomed observables and in the calculation of $\mathcal{B}_2^g(z)$. However, we stress that (cf. Sec. 4) $\mathcal{B}_2^g(z)$ is defined strictly by taking the limit $z_{\text{cut}} \rightarrow 0$ while in the observables considered here one can opt to retain finite z_{cut} effects to improve the accuracy of the calculation. The quantity $\mathcal{B}_2^g(z)$ we have derived applies to both cases with and without finite z_{cut} effects, since these would be captured by the full (numerical) solution of the GFs equations (or equivalently by a NNLL accurate parton shower algorithm).

Using the evolution equation in Eqs. (2.9), (7.1), and following similar steps to those outlined in Appendix D, we obtain the following NNLL results for quark and gluon jets, respectively

$$\begin{aligned} \Sigma^q(v) &= \sigma_0^{Z \rightarrow q\bar{q}} \left(1 + \frac{\alpha_s(E^2)}{2\pi} C_v^{q(1)}(z_{\text{cut}}) \right) e^{-2R_v^q(v, z_{\text{cut}})} \left(1 + \frac{\alpha_s^2(E^2)}{(2\pi)^2} 2\mathcal{F}_{\text{clust}}^q(v) \right), \\ \Sigma^g(v) &= \sigma_0^{H \rightarrow gg} \left(1 + \frac{\alpha_s(E^2)}{2\pi} C_v^{g(1)}(z_{\text{cut}}) \right) e^{-2R_v^g(v, z_{\text{cut}})} \left(1 + \frac{\alpha_s^2(E^2)}{(2\pi)^2} 2\mathcal{F}_{\text{clust}}^g(v) \right). \end{aligned} \quad (8.4)$$

¹²Notice that here we adopt a different normalisation of the observable, compared to Ref. [67], in order to match the corresponding hadron collider jet definitions.

The quantity $R_v(v, z_{\text{cut}})$ denotes the Sudakov radiator, which can be obtained by integrating the inclusive emission probability in Eqs. (2.10), (7.2) with the measurement function of the observables (8.1), (8.2) for a single collinear $a \rightarrow bc$ splitting, namely

$$\Theta(V_x(z, \theta) - v), \quad (8.5)$$

with $V_x = \{FC_x, \lambda_x\}$ and

$$FC_x(z, \theta) \simeq z(1-z)\theta^{2-x}, \quad (8.6)$$

$$\lambda_x(z, \theta) \simeq \min(z, 1-z)\theta^{2-x}, \quad (8.7)$$

where z is the energy fraction of b . This gives (see also Ref. [67]) (with $f \in \{q, g\}$)

$$R_v^f(v, z_{\text{cut}}) \equiv -g_1^f(\lambda_v, \lambda_{z_{\text{cut}}}) - g_2^f(\lambda_v, \lambda_{z_{\text{cut}}}) - h_2^f(\lambda_v) - \frac{\alpha_s}{\pi} h_3^f(\lambda_v; B_{2,v}^f), \quad (8.8)$$

where $\lambda_v \equiv \alpha_s \beta_0 \ln 1/v$, $\lambda_{z_{\text{cut}}} \equiv \alpha_s \beta_0 \ln 1/z_{\text{cut}}$, $\alpha_s \equiv \alpha_s(E^2)$, and

$$\beta_0 = \frac{b_0}{2\pi}. \quad (8.9)$$

The functions in Eq. (8.8) read (we use the notation $C_R^q \equiv C_F$ and $C_R^g \equiv C_A$)

$$g_1^f(\lambda_v, \lambda_{z_{\text{cut}}}) = \frac{C_R^f}{\pi \alpha_s \beta_0^2} \lambda_{z_{\text{cut}}} \ln \left(1 - \frac{2\lambda_v}{2-x} \right), \quad (8.10)$$

$$\begin{aligned} g_2^f(\lambda_v, \lambda_{z_{\text{cut}}}) &= \frac{C_R^f}{\pi \alpha_s \beta_0^2} \lambda_{z_{\text{cut}}}^2 \left(\frac{1-2\lambda_v}{2-x-2\lambda_v} \right) + \frac{C_R^f \beta_1}{\pi \beta_0^3} \lambda_{z_{\text{cut}}} \frac{2\lambda_v + (2-x) \ln \left(1 - \frac{2\lambda_v}{2-x} \right)}{2-x-2\lambda_v} \\ &- \frac{C_R^f}{\pi^2 \beta_0^2} \lambda_{z_{\text{cut}}} \frac{\lambda_v K^{(1)}}{2-x-2\lambda_v}, \end{aligned} \quad (8.11)$$

$$h_2^f(\lambda_v) = \frac{B_1^f}{2\pi \beta_0} \ln \left(1 - \frac{2\lambda_v}{2-x} \right), \quad (8.12)$$

$$\begin{aligned} h_3^f(\lambda_v; B_{2,v}^f) &= \frac{B_1^f \beta_1}{2\beta_0^2 (2-x-2\lambda_v)} \left((2-x) \ln \left(1 - \frac{2\lambda_v}{2-x} \right) + 2\lambda_v \right) \\ &- \frac{B_{2,v}^f}{2\pi \beta_0 (2-x-2\lambda_v)} \lambda_v, \end{aligned} \quad (8.13)$$

where

$$\beta_1 = \frac{17 C_A^2 - 10 C_A T_R n_f - 6 C_F T_R n_f}{24\pi^2}. \quad (8.14)$$

For the observables of interest $B_{2,v}^f$ emerges from the integration of Eqs. (2.10), (7.2) with the phase space constraint in Eq. (8.5) and it is given by

$$B_{2,FC_x}^q = B_{2,\theta^2}^q + C_F b_0 \frac{2}{2-x} \left(3 - \frac{\pi^2}{3} \right) = -\gamma_q^{(2)} + b_0 X_{FC_x}^q, \quad (8.15)$$

$$\begin{aligned} B_{2,FC_x}^g &= B_{2,\theta^2}^g + \frac{b_0}{2-x} \left(C_A \left(\frac{67}{9} - \frac{2\pi^2}{3} \right) - \frac{26}{9} T_R n_f \right) \\ &= -\gamma_g^{(2)} + b_0 X_{FC_x}^g + \frac{1}{2} C_A^2 \left(\frac{4\pi}{3} \text{Cl}_2 \left(\frac{\pi}{3} \right) + h_{\text{clust.}}^{C_A} \right), \end{aligned} \quad (8.16)$$

for the fractional moments of EEC, and

$$B_{2,\lambda_x}^q = B_{2,\theta^2}^q + C_F b_0 \frac{(9 - \pi^2 + 9 \ln 2)}{3(2 - x)} = -\gamma_q^{(2)} + b_0 X_{\lambda_x}^q, \quad (8.17)$$

$$\begin{aligned} B_{2,\lambda_x}^g &= B_{2,\theta^2}^g + \frac{b_0}{2 - x} \left(C_A \left(\frac{137}{36} - \frac{\pi^2}{3} + \frac{44 \ln 2}{12} \right) - T_R n_f \left(\frac{29}{18} + \frac{4 \ln 2}{3} \right) \right) \\ &= -\gamma_g^{(2)} + b_0 X_{\lambda_x}^g + \frac{1}{2} C_A^2 \left(\frac{4}{3} \pi \text{Cl}_2 \left(\frac{\pi}{3} \right) + h_{\text{clust.}}^{C_A} \right), \end{aligned} \quad (8.18)$$

for the WTA angularities. The quantities B_{2,θ^2}^q and B_{2,θ^2}^g are defined in Eqs. (3.6) and (4.2) while X_v^f denotes the observable dependent constants for which we obtain

$$\begin{aligned} X_{FC_x}^q &= C_F \frac{2}{2 - x} \left(3 - \frac{\pi^2}{3} \right) + X_{\theta^2}^q, \\ X_{FC_x}^g &= \frac{1}{2 - x} \left(C_A \left(\frac{67}{9} - \frac{2\pi^2}{3} \right) - \frac{26}{9} T_R n_f \right) + X_{\theta^2}^g, \end{aligned} \quad (8.19)$$

and

$$\begin{aligned} X_{\lambda_x}^q &= C_F \frac{(9 - \pi^2 + 9 \ln 2)}{3(2 - x)} + X_{\theta^2}^q, \\ X_{\lambda_x}^g &= \frac{1}{2 - x} \left(C_A \left(\frac{137}{36} - \frac{\pi^2}{3} + \frac{44 \ln 2}{12} \right) - T_R n_f \left(\frac{29}{18} + \frac{4 \ln 2}{3} \right) \right) + X_{\theta^2}^g, \end{aligned} \quad (8.20)$$

where the constants $X_{\theta^2}^q$ and $X_{\theta^2}^g$ are given in Eqs. (3.7), (7.12). Finally, $h_{\text{clust.}}^{C_A}$ is given in Eq. (7.19). We note that the result for B_{2,λ_x}^q has been previously obtained in Ref. [67].

The clustering corrections $\mathcal{F}_{\text{clust.}}(v)$ in Eq. (8.4) arise from the finite terms $\mathbb{K}_q^{\text{finite}}[G_q, G_g]$ and $\mathbb{K}_g^{\text{finite}}[G_q, G_g]$ in the GF Eqs. (2.9), (7.1) (cf. Appendix C), which give rise to a correction to the Sudakov in Eq. (8.4) and are given by (see also Ref. [67])

$$\begin{aligned} \mathcal{F}_{\text{clust.}}^q(v) &= C_F \left(C_F \frac{4\pi}{3} \text{Cl}_2 \left(\frac{\pi}{3} \right) + C_A h_{\text{clust.}}^{C_A} + T_R n_f h_{\text{clust.}}^{T_R n_f} \right) \frac{\ln v}{2 - x - 2\lambda_v}, \\ \mathcal{F}_{\text{clust.}}^g(v) &= C_A T_R n_f h_{\text{clust.}}^{T_R n_f} \frac{\ln v}{2 - x - 2\lambda_v}, \end{aligned} \quad (8.21)$$

where

$$h_{\text{clust.}}^{T_R n_f} \simeq -1.75559363(5). \quad (8.22)$$

A comment on the difference between quark and gluon jets is in order. This difference can be traced back to the projection (4.1) used in the definition of the inclusive emission probability and hence of $\mathcal{B}_2^f(z)$. As we discussed extensively in the paper, we adopt a different projection for quark and gluon jets due to the more involved structure of collinear singularities in the latter case. This translates into the final anomalous dimensions $B_{2,v}^f$ given in Eqs. (8.15), (8.17). Here we can see that the gluon jet result $B_{2,v}^g$, unlike $B_{2,v}^q$, includes a part of the clustering correction, specifically in the C_A^2 channel (see discussion in Sec. 7.4).

Finally, we comment on the coefficient functions $C_v^{f(1)}(z_{\text{cut}})$ ($f = \{q, g\}$) in Eq. (8.4). These are matching coefficients between the collinear approximation of the generating

functionals and the full $\mathcal{O}(\alpha_s)$ calculation in the limit $v \ll z_{\text{cut}} \ll 1$. For the processes and observables considered here they have the general structure [55]

$$\begin{aligned} C_v^{q(1)}(z_{\text{cut}}) &= H^{q(1)} - 2X_v^q + C_F \left(8 \ln 2 \ln z_{\text{cut}} + 6 \ln 2 - \frac{\pi^2}{3} \right), \\ C_v^{g(1)}(z_{\text{cut}}) &= H^{g(1)} - 2X_v^g + C_A \left(8 \ln 2 \ln z_{\text{cut}} - \frac{\pi^2}{3} \right), \end{aligned} \quad (8.23)$$

where X_v^f are the observable dependent constants of hard-collinear origin given in Eqs. (8.19), (8.20), and the remaining constants are the the (only) process-dependent ingredients of the calculation. Specifically, $H^{f(1)}$ accounts for the hard-virtual corrections at one loop order

$$\begin{aligned} H^{q(1)} &= \pi^2 - 8, \\ H^{g(1)} &= \pi^2. \end{aligned} \quad (8.24)$$

The presence of X_v^f both in Eqs. (8.23) and in Eqs. (8.15), (8.17) indicates that the GF solution is defined in a resummation scheme in which the running of α_s multiplying the constants of collinear origin is absorbed into the anomalous dimensions which define the inclusive emission probability. In alternative approaches to this class of resummations (e.g. that of Refs. [32, 55, 67]) the coupling multiplying these constants is evaluated at the observable-dependent collinear (low) scale, which would remove X_v^f from Eqs. (8.15), (8.17). The physical result at a given logarithmic order is of course resummation-scheme invariant (cf. also footnote 17 in Appendix D).

As a check of our results, we compare the resummed predictions for FC_x and λ_x against the formalism of Refs. [32, 55] adapted to groomed observables in Refs. [66, 67]. Specifically, as observed in Ref. [67], in the case of groomed quark jets the integrated quantities B_{2,λ_x}^q and B_{2,FC_x}^q can be extracted from Sec. 3 of Ref. [55], by combining the endpoint of the two loop DGLAP anomalous dimension $\gamma_f^{(2)}$ with the running of the one-loop hard-collinear constant $C_{\text{hc}}^{(1)}$ and the recoil correction $\delta\mathcal{F}_{\text{rec}}$,¹³ which agrees with our findings in Eqs. (8.15), (8.17). Similarly, an independent calculation of the clustering corrections for quark angularities can be found in Ref. [67]. We also carried out analogous checks for the gluonic results, based on a straightforward extension of the above formalism to $H \rightarrow gg$. We reiterate that, due to the process-independence of the collinear limit, our results can be used for hadron-collider jets after supplying the appropriate process-dependent analogues of the constants in Eqs. (8.23).

9 Conclusions and Outlook

In this paper we have presented a generating functional formulation of the NNLL resummation of collinear logarithms produced by multiple timelike collinear parton splittings. In particular, we have addressed one of the key elements of the generating functionals method,

¹³The hard-collinear correction $\delta\mathcal{F}_{\text{hc}}$ would also contribute for ungroomed angularities and fractional moments of EEC.

namely the Sudakov form factor, which appears in the formalism as the no-branching probability for a given fragmenting parton. We have pointed out that for general NNLL accuracy in the collinear limit, alongside correcting the real emission matrix-element using the triple-collinear splitting functions, the Sudakov form factor also needs to be augmented to the two-loop order. Here we focussed on gluon fragmentation, and have provided the necessary extension by computing the anomalous dimension $\mathcal{B}_2^g(z)$ which governs the intensity of collinear radiation off a gluon as a function of a suitably defined longitudinal momentum fraction z . We envisage that the results presented here will be instrumental to address the following classes of resummation problems:

1. Problems that do not admit a closed-form solution such as, for instance, the differential fragmentation of a jet into a system of microjets. This class of problems is sensitive to the whole non-linear structure of the generating functionals evolution equations provided in this article, which reflects the recursive nature of collinear fragmentation. As such, in the general case only a numerical solution of these equations can be envisioned, which can be achieved either using discretisation techniques or Monte Carlo methods. In particular, our results are necessary for the extension to NNLL of the NLL results of Ref. [7]. We will address some of these aspects in a future publication [1] together with an algorithmic solution to the problem of collinear fragmentation.
2. The second class of collinear problems that can be addressed with the formalism outlined here is that of semi-inclusive observables that are not sensitive to the full non-linear structure of the evolution equations, which can now be solved with analytic methods [73–76, 79–81, 84–86]. Examples of these problems, considered in this article, are groomed event shapes and moments of EEC. We derived new NNLL results for a family of groomed angularities defined w.r.t. the Winner-Take-All axis and fractional moments of energy-energy correlators, which open up a range of interesting phenomenological studies at hadron colliders such as the LHC.
3. Another interesting direction is the extension to more general observables that also exhibit sensitivity to soft physics, including the important cases of ungroomed global event shapes and non-global observables (in the latter case a GFs formulation is given in Refs. [28, 29]). Although many of the above NNLL resummations (e.g. for global event shapes) are known from the literature, their formulation in the GFs language would pave the way for a single resummation tool capable of achieving NNLL accuracy across wide classes of observable. Similar considerations apply to the space-like collinear branching of initial-state partons, which will be a crucial future step. Another key consideration will be the inclusion of spin correlations at NNLL via the use of polarised splitting kernels in the GF evolution equations.

An important additional aspect of the formalism presented here is that it allows one to formulate collinear resummation in a language that resembles that of parton showers, hence offering insight on the design of future NNLL algorithms. For instance, the Sudakov

form factor calculated in this article constitutes a crucial ingredient to reach this perturbative accuracy and it is therefore a key element of future NNLL parton showers. Finally, the results derived in this article are distributed in Mathematica format with the arXiv submission of this paper.

Acknowledgements

We thank Ludovic Scyboz, Gr  gory Soyez and Gavin Salam for useful discussions through the course of this work and comments on the manuscript. Furthermore, we are grateful to Gavin Salam for collaboration on the related forthcoming Ref. [1]. We would also like to thank other colleagues on the PanScales collaboration whose thoughts and efforts towards pushing forward the logarithmic accuracy of parton showers have directly motivated this work. This work has been partly funded by the European Research Council (ERC) under the European Union's Horizon 2020 research and innovation program (grant agreement No 788223) (MvB, MD, BKE and JH) and by the U.K.'s Science and Technologies Facilities Council under grant ST/T001038 (MD). The work of PM is funded by the European Union (ERC, grant agreement No. 101044599, JANUS). Views and opinions expressed are however those of the authors only and do not necessarily reflect those of the European Union or the European Research Council Executive Agency. Neither the European Union nor the granting authority can be held responsible for them.

A Leading order splitting functions

In this appendix we report the well known expression of the unregularised tree-level splitting kernels used in the main text. We factor out the colour factors using the notation

$$P_{qq}(z, \epsilon) = C_F p_{qq}(z, \epsilon), \quad P_{gg}(z) = C_A p_{gg}(z), \quad P_{qg}(z, \epsilon) = T_R n_f p_{qg}(z, \epsilon), \quad (\text{A.1})$$

where the splitting functions in $4 - 2\epsilon$ dimensions read

$$\begin{aligned} p_{qq}(z, \epsilon) &= \frac{1+z^2}{1-z} - \epsilon(1-z), \\ p_{gg}(z) &= \frac{1}{1-z} + \frac{1}{z} - 2 + z(1-z), \\ p_{qg}(z, \epsilon) &= \frac{z^2 + (1-z)^2 - \epsilon}{1-\epsilon}. \end{aligned} \quad (\text{A.2})$$

For the sake of simplicity, in the text we also use the following notation for the $\epsilon = 0$ case

$$\begin{aligned} p_{qq}(z) &\equiv p_{qq}(z, \epsilon = 0), \\ p_{qg}(z) &\equiv p_{qg}(z, \epsilon = 0). \end{aligned} \quad (\text{A.3})$$

B Expression of $\mathcal{B}_2(z)$ for quark fragmentation

The expression of $\mathcal{B}_2^q(z)$ can be organised as follows:¹⁴

$$\mathcal{B}_2^q(z) = C_F^2 \mathcal{B}_2^{q,C_F^2}(z) + C_F C_A \mathcal{B}_2^{q,C_F C_A}(z) + C_F T_R n_f \mathcal{B}_2^{q,C_F T_R}(z) + C_F \left(C_F - \frac{C_A}{2} \right) \mathcal{B}_2^{q,\text{id.}}(z). \quad (\text{B.1})$$

The above functions read

$$\mathcal{B}_2^{q,\text{id.}}(z) = 4z - \frac{7}{2} + \frac{5z^2 - 2}{2(1-z)} \ln z + \frac{1+z^2}{1-z} \left(\frac{\pi^2}{6} - \ln z \ln(1-z) - \text{Li}_2(z) \right), \quad (\text{B.2})$$

$$\mathcal{B}_2^{q,C_F T_R}(z) = -b_0^{(n_f)} p_{qq}(z) \ln z + b_0^{(n_f)} (1-z) - K^{(1),n_f}(1+z) + 2 b_0^{(n_f)} (1+z) \ln(1-z), \quad (\text{B.3})$$

$$\mathcal{B}_2^{q,C_F C_A}(z) = -b_0^{(C_A)} p_{qq}(z) \ln z + b_0^{(C_A)} (1-z) + \frac{3}{2} \frac{z^2 \ln z}{1-z} + \frac{1}{2} (2z-1) \quad (\text{B.4})$$

$$+ 2 b_0^{(C_A)} (1+z) \ln(1-z) + p_{qq}(z) \left(\ln^2 z + \text{Li}_2 \left(\frac{z-1}{z} \right) + 2 \text{Li}_2(1-z) \right) - K^{(1),C_A}(1+z),$$

$$\mathcal{B}_2^{q,C_F^2}(z) = p_{qq}(z) \left(-3 \ln z - 2 \ln z \ln(1-z) + 2 \text{Li}_2 \left(\frac{z-1}{z} \right) \right) - 1 + H^{\text{fin.}}(z), \quad (\text{B.5})$$

where $H^{\text{fin.}}(z)$ is given by a 1-fold integral (*cf.* Figure 4 of ref. [57]), that is provided in Mathematica format as an ancillary file with the arXiv preprint of this article. The function $\mathcal{B}_2^q(z)$ is regular in the soft limit $z \rightarrow 1$ and is thus fully integrable over $z \in [0, 1]$.

C The NNLL $\mathbb{K}^{\text{finite}}$ kernel

In this appendix we report the functions $\mathbb{K}_f^{\text{finite}}$ (with $f \in \{q, g\}$) entering the NNLL evolution equation for the quark generating functionals given in Eqs. (2.9), (7.1). We will start by presenting the result for quark jets due to its simpler structure, and later give the gluon counterpart.

C.1 Quark fragmentation

We can express $\mathbb{K}_q^{\text{finite}}$ as a difference between two terms which encode the (subtracted) real corrections to the first of Eqs. (2.3) and its double counting with the iteration of the NLL kernel, respectively. That is:

$$\mathbb{K}_q^{\text{finite}}[G_q, G_g] \equiv \mathbb{K}_q^R[G_q, G_g] - \mathbb{K}_q^{\text{DC}}[G_q, G_g]. \quad (\text{C.1})$$

The difference of \mathbb{K}_q^R and \mathbb{K}_q^{DC} ensures that the quantity $\mathbb{K}_q^{\text{finite}}$ is infrared finite and purely NNLL.

¹⁴The function $\mathcal{B}_2^q(z)$ computed in Ref. [57] is defined as the $\mathcal{B}_2^q(z)$ used here multiplied by $(\alpha_s/(2\pi))^2$.

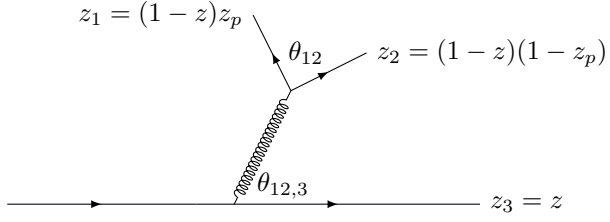


Figure 7: The diagram representing gluon decay to a $q\bar{q}$ pair, where the quark from the gluon decay is either identical or non-identical to the initiating quark.

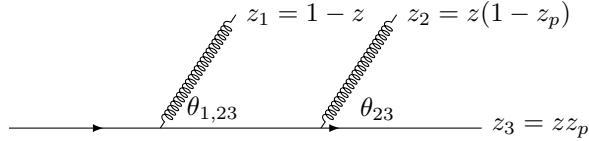


Figure 8: The diagram representing the gluon emission C_F^2 channel.

Following the definition of the inclusive emission probability (2.10) we obtain:

$$\begin{aligned} \mathbb{K}_q^R[G_q, G_g] = & \sum_{(A)} \frac{1}{S_2} \int d\Phi_3^{(A)} P_{1 \rightarrow 3}^{(A)} \left\{ G_{f_1}(x z_p (1-z), t_{1,2}) G_{f_2}(x (1-z_p) (1-z), t_{1,2}) \right. \\ & \times G_q(x z, t_{12,3}) - G_{f_{12}}(x (1-z), t_{12,3}) G_q(x z, t_{12,3}) \left. \right\} \frac{\Delta_q(t)}{\Delta_q(t_{1,2})} \\ & + \int d\Phi_3^{(B)} P_{1 \rightarrow 3}^{(B)} \left\{ G_g(x (1-z), t_{1,23}) G_g(x z (1-z_p), t_{2,3}) \right. \\ & \times G_q(x z z_p, t_{2,3}) - G_g(x (1-z), t_{1,23}) G_q(x z, t_{1,23}) \left. \right\} \frac{\Delta_q(t)}{\Delta_q(t_{2,3})} \Theta(t_{2,3} - t_{1,3}), \quad (C.2) \end{aligned}$$

where we have used the notation $t_{i,j}$ to indicate the value of the evolution time (2.1) corresponding to the angle $\theta_{i,j}$. Moreover, we have parameterised the integrands as ¹⁵

$$P_{1 \rightarrow 3}^{(A)} \equiv \frac{(8\pi)^2}{s_{123}^2} \alpha_s^2 (E^2 g^2(z) \theta_{12,3}^2) \langle \hat{P} \rangle_{C_F C_A, C_F T_R n_f, C_F (C_F - C_A/2)}, \quad (C.3)$$

$$P_{1 \rightarrow 3}^{(B)} \equiv \frac{(8\pi)^2}{s_{123}^2} \alpha_s^2 (E^2 g^2(z) \theta_{1,3}^2) \langle \hat{P} \rangle_{C_F^2}. \quad (C.4)$$

Here, $P_{1 \rightarrow 3}^{(A)}$ is parameterised according to the phase space depicted in Fig. 7, while $P_{1 \rightarrow 3}^{(B)}$ is parameterised according to Fig. 8. The corresponding phase space measures, denoted by $d\Phi_3^{(A,B)}$ in (C.2) are obtained from Eq. (6.1) by setting $\epsilon = 0$ and performing the change of variable (with the corresponding Jacobian) of Figs. 7, 8. The sum in Eq. (C.2) runs over all the (A) colour channels of the type $q \rightarrow f_1 f_2 q(\bar{q})$ defined in Eq. (C.3), and f_i denotes

¹⁵We notice that the production of a $q\bar{q}q$ final state with identical flavours contributing to the $C_F (C_F - C_A/2)$ is finite, and therefore does not factorise into the product of two splitting functions in the strong angular ordered limit.

the flavour of parton i . The factor $1/S_2$ is the symmetry factor to be applied in the case of identical particles (notably $S_2 = 2!$ in the $C_F C_A$ and in the $C_F (C_F - C_A/2)$ channels).

The phase space integrals are now intended to be regulated by the usual cutoff procedure used so far, that implies an upper cut t_0 on evolution time (i.e. a lower cut on angles) and a cut on the energy fractions $1 - z_0 \geq \{z, z_p\} \geq z_0$. All the calculations are then meant to be performed by taking the limit of $t_0 \rightarrow \infty$ and $z_0 \rightarrow 0$ after combining \mathbb{K}_q^R and \mathbb{K}_q^{DC} . We observe that each term in curly brackets in \mathbb{K}_q^R is obtained by subtracting from each real configuration a differential counterterm defined by projecting the real kinematics into a given underlying Born phase space point. Crucially, this requires an infrared-and-collinear-safe definition of the branching variables θ and z , that uniquely specifies the definition of $\mathcal{B}_2^q(z)$. Therefore, the scheme that defines $\mathcal{B}_2^q(z)$ is tightly connected to the specific form of $\mathbb{K}_q^{\text{finite}}[G_q, G_g]$ in Eq. (2.9), which specifically adopts the definition of z and θ of Ref. [57] outlined in Sec. 3. An alternative scheme will modify the expression of both $\mathcal{B}_2^q(z)$ and $\mathbb{K}_q^{\text{finite}}[G_q, G_g]$ by modifying the precise definition of θ and z , but the prediction of the evolution equation is clearly invariant under any scheme change of this type. Following similar considerations for the double-counting term we find

$$\begin{aligned} \mathbb{K}_q^{DC}[G_q, G_g] = & \sum_{g \rightarrow f\bar{f}} \int_t^{t_0} dt_{12,3} dt_{1,2} \int_{z_0}^{1-z_0} dz dz_p P_{qq}(z) P_{fg}(z_p) \left\{ G_f(x z_p (1-z), t_{1,2}) \right. \\ & \times G_f(x (1-z_p) (1-z), t_{1,2}) G_q(x z, t_{12,3}) - G_g(x (1-z), t_{12,3}) G_q(x z, t_{12,3}) \Big\} \\ & \times \frac{\Delta_q(t)}{\Delta_q(t_{1,2})} \Theta(t_{1,2} - t_{12,3}) \\ & + \int_t^{t_0} dt_{1,23} dt_{2,3} \int_{z_0}^{1-z_0} dz dz_p P_{qq}(z) P_{qq}(z_p) \left\{ G_g(x (1-z), t_{1,23}) G_g(x z (1-z_p), t_{2,3}) \right. \\ & \times G_q(x z z_p, t_{2,3}) - G_g(x (1-z), t_{1,23}) G_q(x z, t_{1,23}) \Big\} \frac{\Delta_q(t)}{\Delta_q(t_{2,3})} \Theta(t_{2,3} - t_{1,23}), \quad (\text{C.5}) \end{aligned}$$

where the sum runs over the $g \rightarrow gg$ and $g \rightarrow q\bar{q}$ splitting channels. Eq. (C.5) is obtained by calculating the contribution to Eq. (C.2) due to the iteration of the NLL kernel in Eq. (2.3). We notice that the difference between Eqs. (C.2) and (C.5) (i.e. $\mathbb{K}_q^{\text{finite}}[G_q, G_g]$) only contributes in the regime where all angles are commensurate $t_{2,3} \simeq t_{1,23} \simeq t_{1,3}$. Conversely, $\mathbb{K}_q^{\text{finite}}[G_q, G_g]$ vanishes in the strongly ordered limit. This implies that one can always approximate the angles in the Sudakov and in the GFs according to $t_{2,3} \simeq t_{1,23} \simeq t_{12,3} \simeq t_{1,3}$ neglecting higher-order, N^3LL terms.

C.2 Gluon fragmentation

We now extend the result of the previous section to the case of gluon jets. The derivation proceeds through analogous arguments to the quark case, with two main differences. The first difference is related to the scheme for the anomalous dimension $\mathcal{B}_2^g(z)$ used in the main text for its computation. As we discussed at length in Sec. 4, the definition of $\mathcal{B}_2^g(z)$ relies on a specific projection (4.1) from the three-particle to the two-particle phase space, which is reflected in definition of the inclusive emission probability as well as in the definition of

z and θ used in the calculation of $\mathbb{K}^R[G_q, G_g]$. The latter now reads:

$$\mathbb{K}_g^R[G_q, G_g] = \mathbb{K}_g^{R, C_A T_R}[G_q, G_g] + \mathbb{K}_g^{R, C_F T_R}[G_q, G_g] + \mathbb{K}_g^{R, C_A^2}[G_q, G_g], \quad (C.6)$$

where (using the parameterisation of Figs. 1 and 3)

$$\begin{aligned} \mathbb{K}_g^{R, C_A T_R}[G_q, G_g] &= \int d\Phi_3^{(A)} P_{1 \rightarrow 3}^{C_A T_R} \left\{ G_q(x z_p (1-z), t_{2,3}) G_q(x (1-z_p) (1-z), t_{2,3}) \right. \\ &\quad \times G_g(x z, t_{1,23}) - G_g(x (1-z), t_{1,23}) G_g(x z, t_{1,23}) \left. \right\} \frac{\Delta_g(t)}{\Delta_g(t_{2,3})}, \end{aligned} \quad (C.7)$$

$$\begin{aligned} \mathbb{K}_g^{R, C_F T_R}[G_q, G_g] &= \int d\Phi_3^{(B)} P_{1 \rightarrow 3}^{C_F T_R} \left[\left\{ G_q(x (1-z), t_{2,13}) G_g(x z (1-z_p), t_{1,3}) \right. \right. \\ &\quad \times G_q(x z z_p, t_{1,3}) - G_q(x (1-z), t_{2,13}) G_q(x z, t_{2,13}) \left. \right\} \frac{\Delta_g(t)}{\Delta_g(t_{1,3})} \Theta(t_{1,3} - t_{1,2}) \\ &\quad + \{2 \leftrightarrow 3, z \leftrightarrow 1-z\} \left. \right]. \end{aligned} \quad (C.8)$$

Finally, for the C_A^2 channel we must distinguish between the case in which $z > z_{\text{cut}}$ and $z < z_{\text{cut}}$, following the scheme used to define $\mathcal{B}_2^g(z)$. However, since the latter is defined in the $z_{\text{cut}} \rightarrow 0$ limit, we can entirely neglect the region $z < z_{\text{cut}}$ in the calculation of $\mathbb{K}_g^{R, C_A^2}[G_q, G_g]$. Using the phase space parameterisation of Fig. 4 we then find

$$\mathbb{K}_g^{R, C_A^2}[G_q, G_g] = \mathbb{K}_{g, \{12,3\}}^{R, C_A^2}[G_q, G_g] + \{2 \text{ cyclic permutations}\}, \quad (C.9)$$

where we defined

$$\begin{aligned} \mathbb{K}_{g, \{12,3\}}^{R, C_A^2}[G_q, G_g] &= \frac{1}{2!} \int d\Phi_3^{(A)} P_{1 \rightarrow 3}^{C_A^2} \left\{ G_g(x z_p (1-z), t_{1,2}) G_g(x (1-z_p) (1-z), t_{1,2}) \right. \\ &\quad \times G_g(x z, t_{12,3}) - G_g(x (1-z), t_{12,3}) G_g(x z, t_{12,3}) \left. \right\} \frac{\Delta_g(t)}{\Delta_g(t_{1,2})} \Theta(t_{1,2} - \max\{t_{1,3}, t_{2,3}\}). \end{aligned} \quad (C.10)$$

The additional combinatorial factor $1/2!$ accounts for the remaining two-fold symmetry in the $g \rightarrow ggg$ splitting function.

The second important difference between the gluon and quark cases concerns the double counting term $\mathbb{K}^{\text{DC}}[G_q, G_g]$, which in the gluonic case is more involved due to the fact that two different splitting channels contribute to the NLL evolution equation for G_g (cf. Eq. (2.3)). We write it as

$$\mathbb{K}_g^{\text{DC}}[G_q, G_g] = \mathbb{K}_g^{\text{DC}, C_A T_R}[G_q, G_g] + \mathbb{K}_g^{\text{DC}, C_F T_R}[G_q, G_g] + \mathbb{K}_g^{\text{DC}, C_A^2}[G_q, G_g], \quad (C.11)$$

where (using the parameterisation of Figs. 1, 3 and 4, respectively)¹⁶

$$\begin{aligned} \mathbb{K}_g^{\text{DC}, \text{C}_A \text{T}_R}[G_q, G_g] &= \int_t^{t_0} dt_{1,23} dt_{2,3} \int_{z_0}^{1-z_0} dz dz_p P_{gg}(z) P_{qg}(z_p) \left[\left\{ G_q(x z_p (1-z), t_{2,3}) \right. \right. \\ &\quad \times G_q(x (1-z_p) (1-z), t_{2,3}) G_g(x z, t_{1,23}) - G_g(x (1-z), t_{1,23}) G_g(x z, t_{1,23}) \left. \right\} \\ &\quad \times \frac{\Delta_g(t)}{\Delta_g(t_{2,3})} \Theta(t_{2,3} - t_{1,23}) + \{z \leftrightarrow 1-z\} \left. \right], \end{aligned} \quad (\text{C.12})$$

$$\begin{aligned} \mathbb{K}_g^{\text{DC}, \text{C}_F \text{T}_R}[G_q, G_g] &= \int_t^{t_0} dt_{2,13} dt_{1,3} \int_{z_0}^{1-z_0} dz dz_p P_{qg}(z) P_{qq}(z_p) \left[\left\{ G_q(x (1-z), t_{2,13}) \right. \right. \\ &\quad \times G_g(x z (1-z_p), t_{1,3}) G_q(x z z_p, t_{1,3}) - G_q(x (1-z), t_{2,13}) G_q(x z, t_{2,13}) \left. \right\} \\ &\quad \times \frac{\Delta_g(t)}{\Delta_g(t_{1,3})} \Theta(t_{1,3} - t_{2,13}) + \{2 \leftrightarrow 3, z \leftrightarrow 1-z\} \left. \right], \end{aligned} \quad (\text{C.13})$$

$$\begin{aligned} \mathbb{K}_g^{\text{DC}, \text{C}_A^2}[G_q, G_g] &= \int_t^{t_0} dt_{12,3} dt_{1,2} \int_{z_0}^{1-z_0} dz dz_p P_{gg}(z) P_{gg}(z_p) \left[\left\{ G_g(x z_p (1-z), t_{1,2}) \right. \right. \\ &\quad \times G_g(x (1-z_p) (1-z), t_{1,2}) G_g(x z, t_{12,3}) - G_g(x (1-z), t_{12,3}) G_g(x z, t_{12,3}) \left. \right\} \\ &\quad \times \frac{\Delta_g(t)}{\Delta_g(t_{1,2})} \Theta(t_{1,2} - t_{12,3}) + \{z \leftrightarrow 1-z\} \left. \right]. \end{aligned} \quad (\text{C.14})$$

We note that in Eqs. (C.12) and (C.14) the symmetrisation in $z \leftrightarrow 1-z$ is not accompanied by a factor of $1/2!$ since this is already included in the definition of the leading-order splitting function $P_{gg}(z)$.

D Derivation of $\frac{\theta^2}{\sigma_0} \frac{d^2\sigma}{d\theta^2 dz}$

In this appendix we derive the double-differential distribution in Eq. (D.13). It is instructive to start with the NLL case, for which the distribution $\frac{\theta^2}{\sigma_0} \frac{d^2\sigma}{d\theta^2 dz}$ is defined as (cf. Eq. (2.7))

$$\frac{\theta^2}{\sigma_0} \frac{d^2\sigma^{(f)}}{d\theta^2 dz} = \sum_{m=1}^{\infty} \int dP_m^{(f)} \theta^2 \delta(\theta^2 - \theta_{\text{pass}}^2) \delta(z - z_{\text{pass}}), \quad (\text{D.1})$$

where θ_{pass} and z_{pass} denote the angle and momentum fraction of the largest-angle branching with $1 - z_{\text{cut}} > z_{\text{pass}} > z_{\text{cut}}$. The probabilities $dP_m^{(f)}$ are computed with Eq. (2.2) using the NLL evolution equation (2.3). For the sake of establishing our argument, we consider the simpler case of the fragmentation of a quark. For a given number m of final state

¹⁶We note that the $C_A T_R$ contribution to the double counting term $\mathbb{K}_g^{\text{DC}, \text{C}_A \text{T}_R}[G_q, G_g]$ is symmetric in $z \leftrightarrow 1-z$, while $\mathbb{K}_g^{\text{R}, \text{C}_A \text{T}_R}[G_q, G_g]$ given above is not. This symmetrisation in $\mathbb{K}_g^{\text{R}, \text{C}_A \text{T}_R}[G_q, G_g]$ is not necessary but it could be performed (i.e. adding the same integrand with $z \leftrightarrow 1-z$ and dividing by 2) to mirror the iteration of the NLL kernel.

particles, the observable is defined by considering all sequential primary declusterings with respect to the hard leg that initiates the fragmentation in an angular ordered picture, and setting θ and z to the first one that passes the z_{cut} (with $z_{\text{cut}} \ll 1$) condition. At NLL, each declustering amounts to a single primary emission off the initial hard leg, which then fragments inclusively. Therefore, we can ignore the secondary branchings of the gluons and approximate their generating functional with the first order expansion, that is

$$G_g(x, t) \simeq u. \quad (\text{D.2})$$

With this simplification, the first few terms of the series read

$$\int dP_1^{(q)} = \Delta_q(t), \quad (\text{D.3})$$

$$\int dP_2^{(q)} = \Delta_q(t) \int_t^{t_0} dt_1 \int_{z_0}^{1-z_0} dz_1 P_{qq}(z_1), \quad (\text{D.4})$$

$$\int dP_3^{(q)} = \Delta_q(t) \int_t^{t_0} dt_1 \int_{t_1}^{t_0} dt_2 \int_{z_0}^{1-z_0} dz_1 dz_2 P_{qq}(z_1) P_{qq}(z_2), \quad (\text{D.5})$$

$$\dots = \dots \quad (\text{D.6})$$

The final state with a single parton does not contribute to the distribution (more precisely it contributes a $\delta(\theta^2)$ term), while the final state with two partons (described by $dP_2^{(q)}$) contributes according to the measurement function

$$\theta^2 \delta(\theta^2 - \theta_1^2) \delta(z - z_1) \Theta(z_1 - z_{\text{cut}}). \quad (\text{D.7})$$

Similarly, the state with three partons will involve the measurement function

$$\theta^2 \left(\delta(\theta^2 - \theta_1^2) \delta(z - z_1) \Theta(z_1 - z_{\text{cut}}) + \delta(\theta^2 - \theta_2^2) \delta(z - z_2) \Theta(z_{\text{cut}} - z_1) \Theta(z_2 - z_{\text{cut}}) \right), \quad (\text{D.8})$$

where the first term corresponds to a configuration in which the first, largest-angle emission (declustering) passes the z_{cut} condition, while the second term corresponds to a configuration in which the first emission fails the condition and the observable is then defined by the second branching provided it passes the cut. The configuration in which neither of the declusterings passes the cut only gives a $\delta(\theta^2)$ contribution to the observable, and can be discarded for the differential distribution.

One can then evaluate explicitly the infinite sum in Eq. (D.1) by factoring out the contribution of the branching that passes the cut and summing inclusively over the remaining branchings. If we trade the angular ordering for a $1/n!$ combinatorial factor, we obtain the formula

$$\begin{aligned} \frac{\theta^2}{\sigma_0} \frac{d^2 \sigma^{(f)}}{d\theta^2 dz} &= \Delta_q(t) \frac{\alpha_s(E^2 g(z)^2 \theta^2)}{2\pi} P_{qq}(z) \\ &\times \exp \left\{ \int_t^{t_0} dt' \int_{z_0}^{1-z_0} dz P_{qq}(z) (\Theta(z_{\text{cut}} - z) + \Theta(\theta - \theta') \Theta(z - z_{\text{cut}})) \right\}. \end{aligned} \quad (\text{D.9})$$

We can now evaluate the integral in the exponent and combine it with the Sudakov $\Delta_q(t)$ given in Eq. (2.5). After taking the limits $t_0 \rightarrow \infty$ and $z_0 \rightarrow 0$ we obtain

$$\frac{\theta^2}{\sigma_0} \frac{d^2\sigma^{(f)}}{d\theta^2 dz} = \frac{\alpha_s(E^2 g(z)^2 \theta^2)}{2\pi} P_{qq}(z) e^{-R_q^{\text{NLL}}(\theta, z_{\text{cut}})}, \quad (\text{D.10})$$

where t_θ denotes the evolution time corresponding to the angle θ and

$$R_q^{\text{NLL}}(\theta, z_{\text{cut}}) \equiv \int_0^{t_\theta} dt' \int_{z_{\text{cut}}}^1 dz P_{qq}(z) \quad (\text{D.11})$$

The quantity in the exponent defines the Sudakov radiator featuring in Eq. (D.13). The NNLL version of Eq. (D.10) can be obtained following the same procedure. We start from Eq. (2.7), where now the matching coefficient needs to be evaluated at one loop, that is

$$C(\alpha_s) = 1 + \frac{\alpha_s(E^2)}{2\pi} C_q^{(1)} + \mathcal{O}(\alpha_s^2). \quad (\text{D.12})$$

The constant $C_q^{(1)}$ contains hard-virtual corrections to the Born process, as well as non-logarithmic terms of soft and/or collinear origin that contribute in the limit $\theta \rightarrow 0$.¹⁷

As a second step, we consider the functional derivatives of the NNLL quark generating functional, starting from the term in the first line of Eq. (2.9). The effect of this term is simply to replace P_{qq} in Eq. (D.10) with the full inclusive emission probability $\mathcal{P}_q(z, \theta)$ given in Eqs. (2.9), (2.10). We then consider the contribution of the $\mathbb{K}_q^{\text{finite}}$ term, given in Appendix C. By inspecting the structure of $\mathbb{K}_q^{\text{finite}}$ we observe that the local counterterms in Eqs. (C.2), (C.5) are defined precisely by means of the same projection between the $1 \rightarrow 3$ and the $1 \rightarrow 2$ phase spaces that was used in the definition and calculation of $\mathcal{B}_2^f(z)$. Therefore the observable is defined in exactly the same way for the real contributions as well as for the corresponding counterterms, giving a zero correction. Therefore, the contribution of $\mathbb{K}_q^{\text{finite}}$ to the differential distribution $\frac{\theta^2}{\sigma_0} \frac{d^2\sigma^{(f)}}{d\theta^2 dz}$ vanishes trivially, and one is left with the general form in Eq. (D.13). The same derivation holds for gluon jets, leading to the expression

$$\frac{\theta^2}{\sigma_0} \frac{d^2\sigma}{d\theta^2 dz} = \left(1 + \frac{\alpha_s(E^2)}{2\pi} C_g^{(1)} \right) e^{-R_g^{\text{NNLL}}(\theta, z_{\text{cut}})} \frac{\alpha_s(E^2 g(z)^2 \theta^2)}{2\pi} (\mathcal{P}_{gg}(z, \theta) + \mathcal{P}_{qg}(z, \theta)), \quad (\text{D.13})$$

with

$$R_g^{\text{NNLL}}(\theta, z_{\text{cut}}) \equiv \int_0^{t_\theta} dt' \int_{z_{\text{cut}}}^1 dz (\mathcal{P}_{gg}(z, \theta) + \mathcal{P}_{qg}(z, \theta)), \quad (\text{D.14})$$

¹⁷Importantly, the coupling in Eq. (D.12) is evaluated at the hard scale of the process (i.e. $\mu^2 \sim E^2$), which formally corresponds to working in a resummation scheme [91] in which such non-logarithmic terms are evaluated at the hard scale. In an alternative resummation scheme one may want to calculate some of these non-logarithmic terms (for instance those of soft and/or collinear origin) at the low scales (soft or collinear) of the problem, so that their running generates logarithmic terms at higher perturbative orders. Consistently with a resummation scheme transformation, this implies that the higher-order logarithmic terms generated by the running of the coupling must be subtracted from the anomalous dimension $\mathcal{B}_2^f(z)$ computed here.

where the inclusive emission probabilities are given in Eq. (7.2). In the extraction of $\mathcal{B}_2^g(z)$ we have chosen to work with the fragmentation of a gluon jet defined as one hemisphere in the two-jet limit of the $H \rightarrow gg$ decay in the heavy-top-mass limit. In this case, the one-loop matching coefficient is given by

$$C_g^{(1)} = C_A \left(4 \ln 2 \ln z_{\text{cut}} + \frac{67}{9} - \frac{\pi^2}{3} \right) - T_R n_f \frac{23}{9}. \quad (\text{D.15})$$

E Double-soft end-point contributions to $\mathcal{B}_2^g(z)$

In this appendix we discuss how to devise an alternative scheme for $\mathcal{B}_2^{g,C_A^2}(z)$ in which the clustering and endpoint contributions, whose origin lies in the double-soft limit, completely disappear. The emergence of the clustering correction in Eq. (4.2), and likewise the endpoint contribution in Eq. (7.13), is due to the specific definition of z and θ in the kinematic projection that we used to define $\mathcal{B}_2^{g,C_A^2}(z)$. To make the physics clear it is useful to recapitulate the case of quark jets [57], in which the definition of $\mathcal{B}_2^q(z)$ does not involve such terms. The procedure given in Sec. 4 is based upon decomposing, for each colour channel, the three-particle phase space into angular sectors each containing exactly one collinear singularity. In the case of quark jets, this task is transparent. For correlated channels, there is a unique collinear singularity between the offspring of the gluon decay, and thus there is a single sector defined according to our procedure. For the C_F^2 channel the only collinear singularities arise when emissions g_1 or g_2 are collinear to the quark q_3 , and thus there are two sectors in our procedure. These features lead to a natural definition of z and θ , in all colour channels, that is based on a *naive* clustering procedure in which pairs of partons which do not develop a collinear singularity never get clustered together [57]. An equally valid, albeit tedious, procedure for defining z and θ would be to follow a strict C/A algorithm and define z as the momentum fraction between the two branches produced by the C/A declustering. This procedure would differ from the previous one in finite angular regions resulting in an alternative scheme for $\mathcal{B}_2^q(z)$, which would contain a clustering correction.

Let us now move to the case of gluon jets. As discussed in the main text, the C_A^2 channel has a richer structure of collinear singularities which involves all three partons (gluons) on an equal footing. In particular, it is not possible to separate out correlated and independent emissions. In this case one cannot use the naive clustering argument adopted for quark jets and for this reason we had to resort to strict C/A procedure outlined in the article. This ultimately leads to the appearance of the clustering correction in Eq. (4.2). However, in a situation in which two of the three final state gluons are soft the parent gluon can be uniquely identified and one can separate the double-soft squared amplitude into the sum of correlated and independent emission terms which are identical to those in the quark case up to Casimir scaling.

One could then introduce an alternative scheme in which the double-soft limit is treated as in the quark case, while the hard-collinear leftover is treated as explained in Sec. 4, i.e. using strict C/A declustering. Given that the clustering correction originates from the

double-soft region of phase space, this alternative $\mathcal{B}_2^g(z)$ will directly integrate to

$$\int_0^1 dz \mathcal{B}_2^g(z) = -\gamma_g^{(2)} + b_0 X_\theta^2. \quad (\text{E.1})$$

A scheme of this type has the advantage of eliminating the end-point contribution present in Eq. (7.13), but presents a slight disadvantage in that it makes the calculation of $\mathbb{K}_q^{\text{finite}}$ more cumbersome due to the different projections adopted in the double-soft and in the hard-collinear limits.

Below we present the quantity $\mathcal{B}_2^g(z)$ in this alternate scheme, which differs from the one given in the article exclusively in the C_A^2 colour channel. In order to carry out the computation of $\mathcal{B}_2^{g,C_A^2}(z)$ in the new scheme, we start by separating the double-soft limit of the splitting function, which satisfies Casimir scaling and is therefore identical (up to an overall quadratic Casimir operator) to the quark case. Let gluons (g_i, g_j) be soft, i.e. $z_i, z_j \ll 1$, while parton k is hard $z_k \rightarrow 1$. In the triple-collinear limit we have

$$\langle \hat{P}_{g_i g_j; p_k} \rangle = C_k^2 \langle \hat{P}_{g_i g_j; p_k}^{\text{ind.}} \rangle + C_k C_A \langle \hat{P}_{g_i g_j; p_k}^{\text{corr.}} \rangle, \quad (\text{E.2})$$

where C_k is the Casimir of the hard parton k . The various functions read ¹⁸

$$\langle \hat{P}_{g_i g_j; p_k}^{\text{ind.}} \rangle = \frac{4}{s_{ik} s_{jk}} \frac{z_k}{z_i z_j}, \quad (\text{E.3})$$

and

$$\begin{aligned} \langle \hat{P}_{g_i g_j; p_k}^{\text{corr.}} \rangle &= \frac{(1-\epsilon)}{4z_k(s_{ik} + s_{jk})^2 s_{ij}^2} \left(2 \frac{z_i s_{jk} - z_j s_{ik}}{z_i + z_j} \right)^2 + \frac{1}{s_{ij} s_{ik}} \left(\frac{1}{z_j} + \frac{1}{z_i + z_j} \right) - \frac{1}{2s_{ik} s_{jk}} \frac{z_k}{z_i z_j} \\ &+ \frac{1}{2(s_{ik} + s_{jk}) s_{ij}} \left(\frac{1}{z_i} + \frac{1}{z_j} - \frac{8}{z_i + z_j} \right) - \frac{1}{(s_{ik} + s_{jk}) s_{ik}} \frac{z_k}{z_i (z_i + z_j)} + (i \leftrightarrow j). \end{aligned} \quad (\text{E.4})$$

In the case of three identical gluons, we have to properly symmetrise the double-soft function in order to account for any pair of gluons becoming soft. Therefore we define the following *subtracted* splitting function

$$\langle \hat{P}_{g_1 g_2 g_3}^{\text{sub.}} \rangle \equiv \frac{1}{s_{123}^2} \langle \hat{P}_{g_1 g_2 g_3} \rangle - \langle \hat{P}_{g_1 g_2; g_3} \rangle - \langle \hat{P}_{g_1 g_3; g_2} \rangle - \langle \hat{P}_{g_2 g_3; g_1} \rangle. \quad (\text{E.5})$$

Having removed the double-soft limit, we are now ready to repeat our standard computations using Eq. (E.5) as our integrand, for which we follow the sectorisation introduced in Sec. 4.

The results presented in Sec. 6.3 are then modified as follows:

$$\left(\frac{\theta^2}{\sigma_0} \frac{d^2 \sigma_{\mathcal{R}}^{(2)}}{d\theta^2 dz} \right)_{z_3 > z_{\text{cut}}}^{C_A^2, \text{sub.}} = \left(\frac{C_A \alpha_s}{2\pi} \right)^2 (z(1-z)\theta^2)^{-2\epsilon} \left(H_{\text{soft-coll.}}^{\text{sub.}}(z, \epsilon) + H_{\text{coll.}}^{\text{sub.}}(z, \epsilon) \right. \\ \left. + H_{\text{soft.}}^{\text{sub.}}(z, \epsilon) + H_{\text{fin.}}^{C_A^2, \text{sub.}}(z) \right), \quad (\text{E.6})$$

¹⁸Notice here in particular that we do not send $z_k \rightarrow 1$ in the double-soft splitting functions, because the triple-collinear phase space will be exactly retained when the computation is performed. This choice is made to ensure the subtraction in Eq. (E.5) is achieved locally in phase space.

where

$$\begin{aligned}
H_{\text{soft-coll.}}^{\text{sub.}}(z, \epsilon) &= 4^\epsilon (z^{-2\epsilon} + (1-z)^{-2\epsilon}) (-2 + z(1-z)) \left(\frac{1}{\epsilon^2} + \frac{2 \ln 2}{\epsilon} + 4 \ln^2 2 - \frac{\pi^2}{2} \right), \\
H_{\text{coll.}}^{\text{sub.}}(z, \epsilon) &= 4^\epsilon p_{gg}(z) (z^{-2\epsilon} + (1-z)^{-2\epsilon}) \left[\frac{(11 - 12 \ln 2)}{6\epsilon} + \left(\frac{67}{9} - \frac{\pi^2}{3} - 4 \ln^2 2 \right) \right. \\
&\quad \left. - \frac{11}{6\epsilon} 4^\epsilon \left(\frac{(1-z)^{-2\epsilon}}{1-z} + \frac{z^{-2\epsilon}}{z} \right) + 4^\epsilon (z^{-2\epsilon} + (1-z)^{-2\epsilon}) \frac{2 \ln 2}{z(1-z)\epsilon} \right. \\
&\quad \left. - \frac{1}{z(1-z)} \left(\frac{67}{9} - \frac{2\pi^2}{3} - 8 \ln^2 2 \right) \right], \\
H_{\text{soft}}^{\text{sub.}}(z, \epsilon) &= - (z^{-2\epsilon} + (1-z)^{-2\epsilon}) (-2 + z(1-z)) \left(\frac{2 \ln(2)}{\epsilon} - \frac{h_{\text{pass}}^{\text{sub.}}}{2} \right),
\end{aligned} \tag{E.7}$$

where the constant $h_{\text{soft}}^{\text{sub.}}$ is the result of a 2-fold integration and reads

$$h_{\text{soft}}^{\text{sub.}} \simeq -6.49651797(5). \tag{E.8}$$

The function $H_{\text{fin.}}^{C_A^2, \text{sub.}}$ has the usual decomposition (6.16)

$$H_{\text{fin.}}^{C_A^2, \text{sub.}}(z) = -\frac{11 \ln(2)}{3} \frac{1}{z(1-z)} + G_{z_3 > z_{\text{cut}}}^{\text{sub.}}(z), \tag{E.9}$$

and the remainder function $G_{z_3 > z_{\text{cut}}}^{\text{sub.}}$, see Fig. 9, is integrable in $z \in [0, 1]$ and its integral reads

$$\int_0^1 dz G_{z_3 > z_{\text{cut}}}^{\text{sub.}}(z) \simeq 6.974 \pm 0.001. \tag{E.10}$$

Similarly, below the soft threshold $z_3 < z_{\text{cut}}$ we have

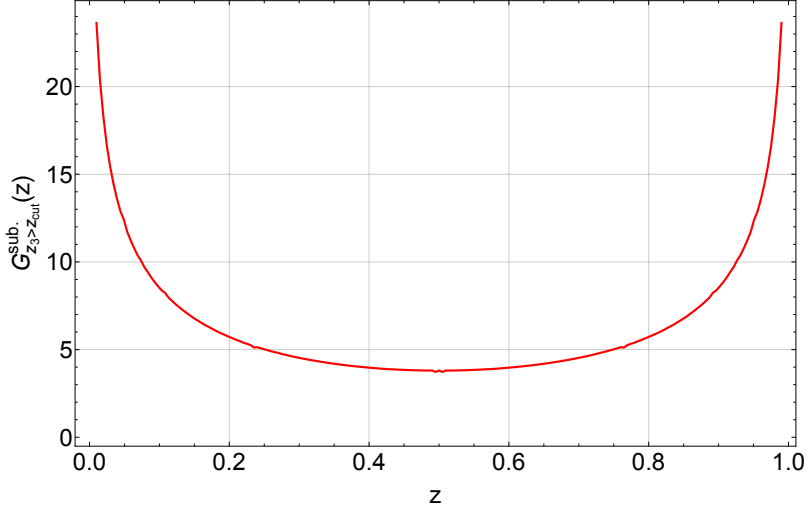


Figure 9: Plot of the function $G_{z_3 > z_{\text{cut}}}^{\text{sub.}}(z)$.

$$\left(\frac{\theta^2}{\sigma_0} \frac{d^2 \sigma_{\mathcal{R}}^{(2)}}{d\theta^2 dz} \right)_{z_3 < z_{\text{cut}}}^{C_A^2, \text{sub.}} = \left(\frac{C_A \alpha_s}{2\pi} \right)^2 (-2 + z(1-z)) \Theta(z - z_{\text{cut}}) \Theta(1 - z_{\text{cut}} - z) \times \\ \times 4^{-\epsilon} (z(1-z))^{-2\epsilon} (\theta^2)^{-\epsilon} \left(\frac{z_{\text{cut}}^{-2\epsilon}}{-\epsilon} \ln \frac{4}{\theta^2} - \frac{\pi^2}{6} - \frac{1}{2} \ln^2 \frac{4}{\theta^2} + h_{\text{fail}}^{pgg} \right), \quad (\text{E.11})$$

where the constant h_{fail}^{pgg} is given in Eq. (6.21). The most important feature of eq. (E.11) is that its z -dependence is fully regular over $z \in [0, 1]$ unlike Eq. (6.20) which contains an end-point contribution.

Finally we compute the pure double-soft contributions, which can be read off from the analytic results of Ref. [57] by enforcing the appropriate limit. Starting with the correlated portion of the double-soft function, eq. (E.4), we find

$$\left(\frac{\theta^2}{\sigma_0} \frac{d^2 \sigma_{\mathcal{R}}^{(2)}}{d\theta^2 dz} \right)^{C_A^2, \text{corr.}} = \left(\frac{C_A \alpha_s}{2\pi} \right)^2 (z(1-z)\theta^2)^{-2\epsilon} \left(\frac{1}{\epsilon^2} + \frac{11}{6\epsilon} - \frac{2\pi^2}{3} + \frac{67}{18} \right) \times \\ \times \left(\frac{(1-z)^{-2\epsilon}}{1-z} + \frac{z^{-2\epsilon}}{z} \right) \Theta(z - z_{\text{cut}}) \Theta(1 - z_{\text{cut}} - z), \quad (\text{E.12})$$

while for the independent emission contribution we get¹⁹

$$\left(\frac{\theta^2}{\sigma_0} \frac{d^2 \sigma_{\mathcal{R}}^{(2)}}{d\theta^2 dz} \right)^{C_A^2, \text{ind.}} = \left(\frac{C_A \alpha_s}{2\pi} \right)^2 (z(1-z)\theta^2)^{-2\epsilon} \left(\frac{1}{\epsilon^2} - \frac{5\pi^2}{6} \right) \left(\frac{z^{-2\epsilon}}{1-z} + \frac{(1-z)^{-2\epsilon}}{z} \right) \times \\ \times \Theta(z - z_{\text{cut}}) \Theta(1 - z_{\text{cut}} - z) \\ + \left(\frac{C_A \alpha_s}{2\pi} \right)^2 \frac{1}{z(1-z)} \Theta(z - z_{\text{cut}}) \Theta(1 - z_{\text{cut}} - z) \times \\ \times 4^{-\epsilon} (z(1-z))^{-2\epsilon} (\theta^2)^{-\epsilon} \left(\frac{z_{\text{cut}}^{-2\epsilon}}{-\epsilon} \ln \frac{4}{\theta^2} - \frac{\pi^2}{6} - \frac{1}{2} \ln^2 \frac{4}{\theta^2} \right). \quad (\text{E.13})$$

Adding all the results in Eqs. (E.6), (E.11), (E.12), (E.13), and the relevant virtual corrections, the alternative scheme yields

$$\mathcal{B}_2^{g, C_A^2, \text{alt.}}(z) = G_{z_3 > z_{\text{cut}}}^{\text{sub.}}(z) + \mathcal{B}_2^{g, C_A^2, \text{analytic, alt.}}(z), \quad (\text{E.14})$$

where

$$\mathcal{B}_2^{g, C_A^2, \text{analytic, alt.}}(z) = \frac{1}{18} (2 - z(1-z)) \left(-18 h_{\text{soft}}^{\text{sub.}} - 18 h_{\text{fail}}^{pgg} + 6\pi^2 - 132 \ln 2 - 72 \ln^2 2 \right) \\ + \frac{-265 + 134z - 134z^2}{18} + \frac{11(1 - 3z + 2z^2 - z^3)}{6(1-z)} \ln z \\ + \frac{11(-1 + 2z - z^2 + z^3)}{6z} \ln(1-z) - \frac{11}{6} \frac{\ln z}{1-z} - \frac{11}{6} \frac{\ln(1-z)}{z} \\ - 2 p_{gg}(z) \ln(1-z) \ln z + \frac{11}{6} (2 - z(1-z)) \ln(z(1-z)). \quad (\text{E.15})$$

¹⁹The third line of Eq. (E.13) emerges when the gluon at larger angle fails the z_{cut} condition. Although this contribution can not be extracted directly from Ref. [57], it entails a straightforward computation.

The integral of $\mathcal{B}_2^{g, C_A^2, \text{alt.}}(z)$ then reads

$$\int_0^1 dz \mathcal{B}_2^{g, C_A^2, \text{alt.}}(z) \simeq -7.858 \pm 0.001. \quad (\text{E.16})$$

It is easy to verify that eq. (E.16) agrees with the sum rule given in Eq. (E.1).

References

- [1] M. van Beekveld, M. Dasgupta, B. El-Menoufi, J. Helliwell, P. Monni and G. P. Salam, *In preparation*, .
- [2] K. Konishi, A. Ukawa and G. Veneziano, *Jet Calculus: A Simple Algorithm for Resolving QCD Jets*, *Nucl. Phys. B* **157** (1979) 45–107.
- [3] A. Bassetto, M. Ciafaloni and G. Marchesini, *Jet Structure and Infrared Sensitive Quantities in Perturbative QCD*, *Phys. Rept.* **100** (1983) 201–272.
- [4] Y. L. Dokshitzer, V. A. Khoze, A. H. Mueller and S. I. Troian, *Basics of perturbative QCD*. 1991.
- [5] R. K. Ellis, W. J. Stirling and B. R. Webber, *QCD and collider physics*, vol. 8. Cambridge University Press, 2, 2011. 10.1017/CBO9780511628788.
- [6] J. M. Campbell et al., *Event Generators for High-Energy Physics Experiments*, in *Snowmass 2021*, 3, 2022. [2203.11110](#).
- [7] M. Dasgupta, F. Dreyer, G. P. Salam and G. Soyez, *Small-radius jets to all orders in QCD*, *JHEP* **04** (2015) 039, [\[1411.5182\]](#).
- [8] Z.-B. Kang, F. Ringer and I. Vitev, *The semi-inclusive jet function in SCET and small radius resummation for inclusive jet production*, *JHEP* **10** (2016) 125, [\[1606.06732\]](#).
- [9] A. Jain, M. Procura and W. J. Waalewijn, *Parton Fragmentation within an Identified Jet at NNLL*, *JHEP* **05** (2011) 035, [\[1101.4953\]](#).
- [10] H.-M. Chang, M. Procura, J. Thaler and W. J. Waalewijn, *Calculating Track-Based Observables for the LHC*, *Phys. Rev. Lett.* **111** (2013) 102002, [\[1303.6637\]](#).
- [11] M. Ritzmann and W. J. Waalewijn, *Fragmentation in Jets at NNLO*, *Phys. Rev. D* **90** (2014) 054029, [\[1407.3272\]](#).
- [12] B. T. Elder, M. Procura, J. Thaler, W. J. Waalewijn and K. Zhou, *Generalized Fragmentation Functions for Fractal Jet Observables*, *JHEP* **06** (2017) 085, [\[1704.05456\]](#).
- [13] H. Chen, I. Moult and H. X. Zhu, *Quantum Interference in Jet Substructure from Spinning Gluons*, *Phys. Rev. Lett.* **126** (2021) 112003, [\[2111.02492\]](#).
- [14] D. Neill and F. Ringer, *Soft Fragmentation on the Celestial Sphere*, *JHEP* **06** (2020) 086, [\[2003.02275\]](#).
- [15] H. Chen, I. Moult and H. X. Zhu, *Spinning gluons from the QCD light-ray OPE*, *JHEP* **08** (2022) 233, [\[2104.00009\]](#).
- [16] D. Neill, F. Ringer and N. Sato, *Leading jets and energy loss*, *JHEP* **07** (2021) 041, [\[2103.16573\]](#).
- [17] H. Chen, I. Moult, J. Sandor and H. X. Zhu, *Celestial blocks and transverse spin in the three-point energy correlator*, *JHEP* **09** (2022) 199, [\[2202.04085\]](#).

[18] H. Chen, M. Jaarsma, Y. Li, I. Moult, W. J. Waalewijn and H. X. Zhu, *Collinear Parton Dynamics Beyond DGLAP*, [2210.10061](#).

[19] W. Chen, J. Gao, Y. Li, Z. Xu, X. Zhang and H. X. Zhu, *NNLL Resummation for Projected Three-Point Energy Correlator*, [2307.07510](#).

[20] M. Dasgupta and G. P. Salam, *Resummation of nonglobal QCD observables*, *Phys. Lett. B* **512** (2001) 323–330, [[hep-ph/0104277](#)].

[21] A. Banfi, G. Marchesini and G. Smye, *Away from jet energy flow*, *JHEP* **08** (2002) 006, [[hep-ph/0206076](#)].

[22] Y. Hatta and T. Ueda, *Resummation of non-global logarithms at finite N_c* , *Nucl. Phys. B* **874** (2013) 808–820, [[1304.6930](#)].

[23] S. Caron-Huot, *Resummation of non-global logarithms and the BFKL equation*, *JHEP* **03** (2018) 036, [[1501.03754](#)].

[24] A. J. Larkoski, I. Moult and D. Neill, *Non-Global Logarithms, Factorization, and the Soft Substructure of Jets*, *JHEP* **09** (2015) 143, [[1501.04596](#)].

[25] D. Neill, *The Asymptotic Form of Non-Global Logarithms, Black Disc Saturation, and Gluonic Deserts*, *JHEP* **01** (2017) 109, [[1610.02031](#)].

[26] R. Ángeles Martínez, M. De Angelis, J. R. Forshaw, S. Plätzer and M. H. Seymour, *Soft gluon evolution and non-global logarithms*, *JHEP* **05** (2018) 044, [[1802.08531](#)].

[27] Y. Hatta and T. Ueda, *Non-global logarithms in hadron collisions at $N_c = 3$* , *Nucl. Phys. B* **962** (2021) 115273, [[2011.04154](#)].

[28] A. Banfi, F. A. Dreyer and P. F. Monni, *Higher-order non-global logarithms from jet calculus*, *JHEP* **03** (2022) 135, [[2111.02413](#)].

[29] A. Banfi, F. A. Dreyer and P. F. Monni, *Next-to-leading non-global logarithms in QCD*, *JHEP* **10** (2021) 006, [[2104.06416](#)].

[30] T. Becher, N. Schalch and X. Xu, *Resummation of Next-to-Leading Non-Global Logarithms at the LHC*, [2307.02283](#).

[31] A. Banfi, G. P. Salam and G. Zanderighi, *Semi-numerical resummation of event shapes*, *JHEP* **01** (2002) 018, [[hep-ph/0112156](#)].

[32] A. Banfi, H. McAslan, P. F. Monni and G. Zanderighi, *A general method for the resummation of event-shape distributions in e^+e^- annihilation*, *JHEP* **05** (2015) 102, [[1412.2126](#)].

[33] A. Banfi, H. McAslan, P. F. Monni and G. Zanderighi, *The two-jet rate in e^+e^- at next-to-next-to-leading-logarithmic order*, *Phys. Rev. Lett.* **117** (2016) 172001, [[1607.03111](#)].

[34] H. T. Li and P. Skands, *A framework for second-order parton showers*, *Phys. Lett. B* **771** (2017) 59–66, [[1611.00013](#)].

[35] S. Höche, F. Krauss and S. Prestel, *Implementing NLO DGLAP evolution in Parton Showers*, *JHEP* **10** (2017) 093, [[1705.00982](#)].

[36] M. Dasgupta, F. A. Dreyer, K. Hamilton, P. F. Monni and G. P. Salam, *Logarithmic accuracy of parton showers: a fixed-order study*, *JHEP* **09** (2018) 033, [[1805.09327](#)].

[37] F. Dulat, S. Höche and S. Prestel, *Leading-Color Fully Differential Two-Loop Soft Corrections to QCD Dipole Showers*, *Phys. Rev. D* **98** (2018) 074013, [[1805.03757](#)].

[38] G. Bewick, S. Ferrario Ravasio, P. Richardson and M. H. Seymour, *Logarithmic accuracy of angular-ordered parton showers*, *JHEP* **04** (2020) 019, [[1904.11866](#)].

[39] J. R. Forshaw, J. Holguin and S. Plätzer, *Parton branching at amplitude level*, *JHEP* **08** (2019) 145, [[1905.08686](#)].

[40] M. Dasgupta, F. A. Dreyer, K. Hamilton, P. F. Monni, G. P. Salam and G. Soyez, *Parton showers beyond leading logarithmic accuracy*, *Phys. Rev. Lett.* **125** (2020) 052002, [[2002.11114](#)].

[41] J. R. Forshaw, J. Holguin and S. Plätzer, *Building a consistent parton shower*, *JHEP* **09** (2020) 014, [[2003.06400](#)].

[42] K. Hamilton, R. Medves, G. P. Salam, L. Scyboz and G. Soyez, *Colour and logarithmic accuracy in final-state parton showers*, *JHEP* **03** (2021) 041, [[2011.10054](#)].

[43] Z. Nagy and D. E. Soper, *Summations of large logarithms by parton showers*, *Phys. Rev. D* **104** (2021) 054049, [[2011.04773](#)].

[44] Z. Nagy and D. E. Soper, *Summations by parton showers of large logarithms in electron-positron annihilation*, [2011.04777](#).

[45] K. Hamilton, A. Karlberg, G. P. Salam, L. Scyboz and R. Verheyen, *Soft spin correlations in final-state parton showers*, *JHEP* **03** (2022) 193, [[2111.01161](#)].

[46] A. Karlberg, G. P. Salam, L. Scyboz and R. Verheyen, *Spin correlations in final-state parton showers and jet observables*, *Eur. Phys. J. C* **81** (2021) 681, [[2103.16526](#)].

[47] F. Herren, S. Höche, F. Krauss, D. Reichelt and M. Schoenherr, *A new approach to color-coherent parton evolution*, [2208.06057](#).

[48] M. van Beekveld, S. Ferrario Ravasio, G. P. Salam, A. Soto-Ontoso, G. Soyez and R. Verheyen, *PanScales parton showers for hadron collisions: formulation and fixed-order studies*, *JHEP* **11** (2022) 019, [[2205.02237](#)].

[49] M. van Beekveld, S. Ferrario Ravasio, K. Hamilton, G. P. Salam, A. Soto-Ontoso, G. Soyez et al., *PanScales showers for hadron collisions: all-order validation*, *JHEP* **11** (2022) 020, [[2207.09467](#)].

[50] K. Hamilton, A. Karlberg, G. P. Salam, L. Scyboz and R. Verheyen, *Matching and event-shape NNLO accuracy in parton showers*, *JHEP* **03** (2023) 224, [[2301.09645](#)].

[51] M. van Beekveld and S. Ferrario Ravasio, *Next-to-leading-logarithmic PanScales showers for Deep Inelastic Scattering and Vector Boson Fusion*, [2305.08645](#).

[52] B. Assi and S. Höche, *A new approach to QCD evolution in processes with massive partons*, [2307.00728](#).

[53] S. F. Ravasio, K. Hamilton, A. Karlberg, G. P. Salam, L. Scyboz and G. Soyez, *A parton shower with higher-logarithmic accuracy for soft emissions*, [2307.11142](#).

[54] S. Catani, B. R. Webber and G. Marchesini, *QCD coherent branching and semiinclusive processes at large x* , *Nucl. Phys. B* **349** (1991) 635–654.

[55] A. Banfi, B. K. El-Menoufi and P. F. Monni, *The Sudakov radiator for jet observables and the soft physical coupling*, *JHEP* **01** (2019) 083, [[1807.11487](#)].

[56] S. Catani, D. De Florian and M. Grazzini, *Soft-gluon effective coupling and cusp anomalous dimension*, *Eur. Phys. J. C* **79** (2019) 685, [[1904.10365](#)].

[57] M. Dasgupta and B. K. El-Menoufi, *Dissecting the collinear structure of quark splitting at NNLL*, *JHEP* **12** (2021) 158, [[2109.07496](#)].

[58] A. Banfi, G. P. Salam and G. Zanderighi, *Principles of general final-state resummation and automated implementation*, *JHEP* **03** (2005) 073, [[hep-ph/0407286](#)].

[59] C. F. Berger, T. Kucs and G. F. Sterman, *Event shape / energy flow correlations*, *Phys. Rev. D* **68** (2003) 014012, [[hep-ph/0303051](#)].

[60] M. Dasgupta, A. Fregoso, S. Marzani and G. P. Salam, *Towards an understanding of jet substructure*, *JHEP* **09** (2013) 029, [[1307.0007](#)].

[61] A. J. Larkoski, S. Marzani, G. Soyez and J. Thaler, *Soft Drop*, *JHEP* **05** (2014) 146, [[1402.2657](#)].

[62] J. M. Campbell and E. W. N. Glover, *Double unresolved approximations to multiparton scattering amplitudes*, *Nucl. Phys. B* **527** (1998) 264–288, [[hep-ph/9710255](#)].

[63] S. Catani and M. Grazzini, *Collinear factorization and splitting functions for next-to-next-to-leading order QCD calculations*, *Phys. Lett. B* **446** (1999) 143–152, [[hep-ph/9810389](#)].

[64] O. Braun-White and N. Glover, *Decomposition of triple collinear splitting functions*, *JHEP* **09** (2022) 059, [[2204.10755](#)].

[65] G. F. R. Sborlini, D. de Florian and G. Rodrigo, *Double collinear splitting amplitudes at next-to-leading order*, *JHEP* **01** (2014) 018, [[1310.6841](#)].

[66] D. Anderle, M. Dasgupta, B. K. El-Menoufi, J. Helliwell and M. Guzzi, *Groomed jet mass as a direct probe of collinear parton dynamics*, *Eur. Phys. J. C* **80** (2020) 827, [[2007.10355](#)].

[67] M. Dasgupta, B. K. El-Menoufi and J. Helliwell, *QCD resummation for groomed jet observables at NNLL+NLO*, *JHEP* **01** (2023) 045, [[2211.03820](#)].

[68] C. T. H. Davies and W. J. Stirling, *Nonleading Corrections to the Drell-Yan Cross-Section at Small Transverse Momentum*, *Nucl. Phys. B* **244** (1984) 337–348.

[69] D. de Florian and M. Grazzini, *The Structure of large logarithmic corrections at small transverse momentum in hadronic collisions*, *Nucl. Phys. B* **616** (2001) 247–285, [[hep-ph/0108273](#)].

[70] D. de Florian and M. Grazzini, *The Back-to-back region in $e^+ e^-$ energy-energy correlation*, *Nucl. Phys. B* **704** (2005) 387–403, [[hep-ph/0407241](#)].

[71] S. Catani, *The Singular behavior of QCD amplitudes at two loop order*, *Phys. Lett. B* **427** (1998) 161–171, [[hep-ph/9802439](#)].

[72] A. Gehrmann-De Ridder and E. W. N. Glover, *A Complete $O(\alpha_s \alpha_s)$ calculation of the photon + 1 jet rate in $e^+ e^-$ annihilation*, *Nucl. Phys. B* **517** (1998) 269–323, [[hep-ph/9707224](#)].

[73] C. Frye, A. J. Larkoski, M. D. Schwartz and K. Yan, *Factorization for groomed jet substructure beyond the next-to-leading logarithm*, *JHEP* **07** (2016) 064, [[1603.09338](#)].

[74] C. Frye, A. J. Larkoski, M. D. Schwartz and K. Yan, *Precision physics with pile-up insensitive observables*, [1603.06375](#).

[75] A. Larkoski, S. Marzani, J. Thaler, A. Tripathi and W. Xue, *Exposing the QCD Splitting Function with CMS Open Data*, *Phys. Rev. Lett.* **119** (2017) 132003, [[1704.05066](#)].

[76] S. Marzani, L. Schunk and G. Soyez, *The jet mass distribution after Soft Drop*, *Eur. Phys. J. C* **78** (2018) 96, [[1712.05105](#)].

[77] CMS collaboration, A. M. Sirunyan et al., *Measurements of the differential jet cross section as a function of the jet mass in dijet events from proton-proton collisions at $\sqrt{s} = 13$ TeV*, *JHEP* **11** (2018) 113, [[1807.05974](#)].

[78] ATLAS collaboration, G. Aad et al., *Measurement of soft-drop jet observables in pp collisions with the ATLAS detector at $\sqrt{s} = 13$ TeV*, *Phys. Rev. D* **101** (2020) 052007, [[1912.09837](#)].

[79] S. Marzani, D. Reichelt, S. Schumann, G. Soyez and V. Theeuwes, *Fitting the Strong Coupling Constant with Soft-Drop Thrust*, *JHEP* **11** (2019) 179, [[1906.10504](#)].

[80] A. Kardos, A. J. Larkoski and Z. Trócsányi, *Groomed jet mass at high precision*, *Phys. Lett. B* **809** (2020) 135704, [[2002.00942](#)].

[81] A. Kardos, A. J. Larkoski and Z. Trócsányi, *Two- and three-loop data for the groomed jet mass*, *Phys. Rev. D* **101** (2020) 114034, [[2002.05730](#)].

[82] CMS collaboration, *Study of quark and gluon jet substructure in dijet and Z+jet events from pp collisions*, .

[83] P. Cal, K. Lee, F. Ringer and W. J. Waalewijn, *The soft drop momentum sharing fraction zg beyond leading-logarithmic accuracy*, *Phys. Lett. B* **833** (2022) 137390, [[2106.04589](#)].

[84] S. Caletti, O. Fedkevych, S. Marzani, D. Reichelt, S. Schumann, G. Soyez et al., *Jet angularities in Z+jet production at the LHC*, *JHEP* **07** (2021) 076, [[2104.06920](#)].

[85] D. Reichelt, S. Caletti, O. Fedkevych, S. Marzani, S. Schumann and G. Soyez, *Phenomenology of jet angularities at the LHC*, *JHEP* **03** (2022) 131, [[2112.09545](#)].

[86] H. S. Hannesdottir, A. Pathak, M. D. Schwartz and I. W. Stewart, *Prospects for strong coupling measurement at hadron colliders using soft-drop jet mass*, [2210.04901](#).

[87] A. J. Larkoski, D. Neill and J. Thaler, *Jet Shapes with the Broadening Axis*, *JHEP* **04** (2014) 017, [[1401.2158](#)].

[88] G. Bell, A. Hornig, C. Lee and J. Talbert, *e^+e^- angularity distributions at NNLL' accuracy*, *JHEP* **01** (2019) 147, [[1808.07867](#)].

[89] M. Procura, W. J. Waalewijn and L. Zeune, *Joint resummation of two angularities at next-to-next-to-leading logarithmic order*, *JHEP* **10** (2018) 098, [[1806.10622](#)].

[90] C. W. Bauer, A. V. Manohar and P. F. Monni, *Disentangling observable dependence in $SCET_I$ and $SCET_{II}$ anomalous dimensions: angularities at two loops*, *JHEP* **07** (2021) 214, [[2012.09213](#)].

[91] S. Catani, D. de Florian and M. Grazzini, *Universality of nonleading logarithmic contributions in transverse momentum distributions*, *Nucl. Phys. B* **596** (2001) 299–312, [[hep-ph/0008184](#)].